Seminar Report Entitled

FILM COOLING USING TRENCHED HOLES

In Partial Fulfilment of Credit Seminar

ME 694

Submitted by

Sanit Prashant Bhatkar

173109003

Department of Mechanical Engineering

INDIAN INSTITUTE OF TECHNOLOGY BOMBAY

2018

ABSTRACT

Gas turbines are used in engineering applications for generation of power. With the increasing need for electricity, engineers have to increase the efficiency and maximum power output, thus increasing the working temperature of the turbine. The temperature of the combustion gas can induce thermal stresses on the turbine blade causing them to fail. The external cooling technique such as film cooling is used to keep the metal temperature within permissible limits.

Film cooling is achieved by drilling the holes on the turbine blade and passing the coolant gas through the holes. The geometry of the hole and the flow conditions significantly affect the effectiveness of the film cooling. This report presents a summary of the available reported literature in the film cooling technology. The film cooling with a trench is the type of film cooling in which the shallow slots are machined on the surface of the turbine blade and the coolant is injected in the trench. Effects of the various flow and geometry parameters on the effectiveness are discussed in the report.

CFD and the experiments are the two methods used to understand the physics of the problem. Different flow measurement methods and various numerical models for defining turbulence are discussed in the report. The simple cylindrical configuration is compared with the shaped, and the trenched hole for the optimum choice of cooling hole arrangement.

Keywords: Gas turbines, Film cooling, Trenched holes

CONTENTS

LIST OF FIGURES

LIST OF TABLES

NOMENCLATURE

η	Adiabatic effectiveness
q''	Heat transfer rate per unit area
h	Heat transfer coefficient
M	Blowing ratio
I	Momentum flux
c	Mass concentration
D	Diameter of the coolant hole
P	Pitch representing the distance between two holes
L	Length of the coolant hole
X	Longitudinal distance from the origin on the airfoil
Z	Lateral distance from the origin on the airfoil
T	Temperature
U	Velocity
ρ	Density
D.R.	Density Ratio
Tu	Turbulence intensity
μ	Viscosity
Pr	Prandtl number
τ	Shear stress

Subscripts:

∞	Mainstream flow parameter
aw	Adiabatic wall condition
m	Airfoil metal temperature
f	Film parameter
c	Coolant parameter

Chapter 1
INTRODUCTION

1.1 Introduction

Gas turbines engines are widely to propel aircraft, tanks, and large naval ships and also to provide electrical power. New technologies are being developed to increase the efficiency of the turbine engine by allowing the gas entering the turbine to have high temperature values. The higher temperature of the gases results in improved thermal efficiency and power output. The temperature of the gases can exceed the allowable metal temperatures of the turbine blades thereby inducing thermal stresses on the airfoil. The failure of the airfoil due to the thermal stress is mitigated by cooling the surface with several methodologies. Film cooling is one of the surface cooling technology which involves bleeding of coolant through the holes drilled on the surface of the airfoil. The film cooling is applied to all regions of airfoil namely leading edge, trailing edge and the curved surface.

1.2 Basic definitions

Adiabatic wall temperature

The purpose of the film cooling is to reduce the local temperature near the surface of the airfoil. The heat transfer from air to the surface of airfoil is good indicator of the cooling effect. The heat transfer can be given by the convection heat transfer equation 1. The choice of the reference temperature in Eq.1 is important. The coolant temperature T_c cannot be used as a reference as the coolant mixes with the mainstream causing variation in local fluid temperature along the downstream.

$$q'' = h_f \left(T_{ref} - T_{wall} \right) \qquad (1)$$

If the free stream temperature T_∞ is used as a reference, the heat transfer coefficient varies with free stream flow conditions. Thus the temperature immediately above the adiabatic surface is used as a reference and it is called as adiabatic wall temperature T_{aw}.

Adiabatic effectiveness

It is difficult to simulate the real turbine conditions in an experiment. Thus the simplified model of the film cooling is studied to understand the effect of various parameters on the film cooling performance. To compare the results of the experiment with the real turbine conditions, the adiabatic wall temperature is expressed in terms of dimensionless parameter η called as adiabatic effectiveness given by the Eq.2. $T_{c,exit}$ is the temperature of the coolant at the exit of the hole.

$$\eta = \frac{T_\infty - T_{aw}}{T_\infty - T_{c,exit}} \qquad (2)$$

The adiabatic effectiveness varies with various parameters like geometry of the hole, curvature of the airfoil, rotation of the turbine etc. Adiabatic effectiveness gives good indication for choosing the correct configuration for the film cooling.

Overall effectiveness

The airfoil metal temperature T_m depends on internal as well as external film cooling. The overall effectiveness ϕ is the non-dimensional parameter indicating the actual metal temperature of the airfoil and it is given by Eq.3. Overall effectiveness is the indicator of the effectiveness of the all the cooling arrangements used for the airfoil.

$$\phi = \frac{T_\infty - T_m}{T_\infty - T_{c,inlet}} \qquad (3)$$

Net heat flux reduction

The net heat flux reduction Δq_r is defined as the heat transfer that occurs without film cooling $q_{\mathbf{o}}''$ relative to that with the film cooling q_f'' and given by Eq.4. Whether or not to use film cooling on a particular location is assessed by the total reduction in the net heat flux. The net heat reduction can be expressed in terms of adiabatic and overall effectiveness.

$$\Delta q_r = 1 - \frac{q_{\mathrm{O}}''}{q_f''} = 1 - \frac{h_f (T_{aw} - T_w)}{h_{\mathrm{O}} (T_\infty - T_w)} = 1 - \frac{h_f}{h_{\mathrm{O}}} \left(\frac{1-\eta}{\phi} \right) \qquad (4)$$

Blowing ratio

Blowing ratio is the ratio of mass flux of coolant gas to the mainstream gas, and it is defined by Eq.5

$$M = \frac{\rho_c U_c}{\rho_\infty U_\infty} \qquad (5)$$

Density ratio

Density ratio is the ratio of the density of coolant gas to the mainstream gas, and it is defined by Eq.6

$$D.R. = \frac{\rho_c}{\rho_\infty} \qquad (6)$$

1.3 Objective

The objectives of the study are:

1. Understand the flow physics of film cooling and the effect of various parameters on the performance of the film cooling.
2. Study different film cooling configurations.

Chapter 2
FILM COOLING DESCRIPTION

2.1 Introduction

In an ideal case such as case (a) of Fig.1, the coolant ejected from the drilled holes remains attached to the surface of the airfoil without mixing with the mainstream flow. Effectiveness η for the ideal case is one. In a real-world application, there is turbulent mixing of the coolant gas with the mainstream. There are various parameters like the hole geometry, shape of the airfoil, mass flux ratio affecting the effectiveness of the film cooling. The individual effect of these parameters is discussed in the chapter.

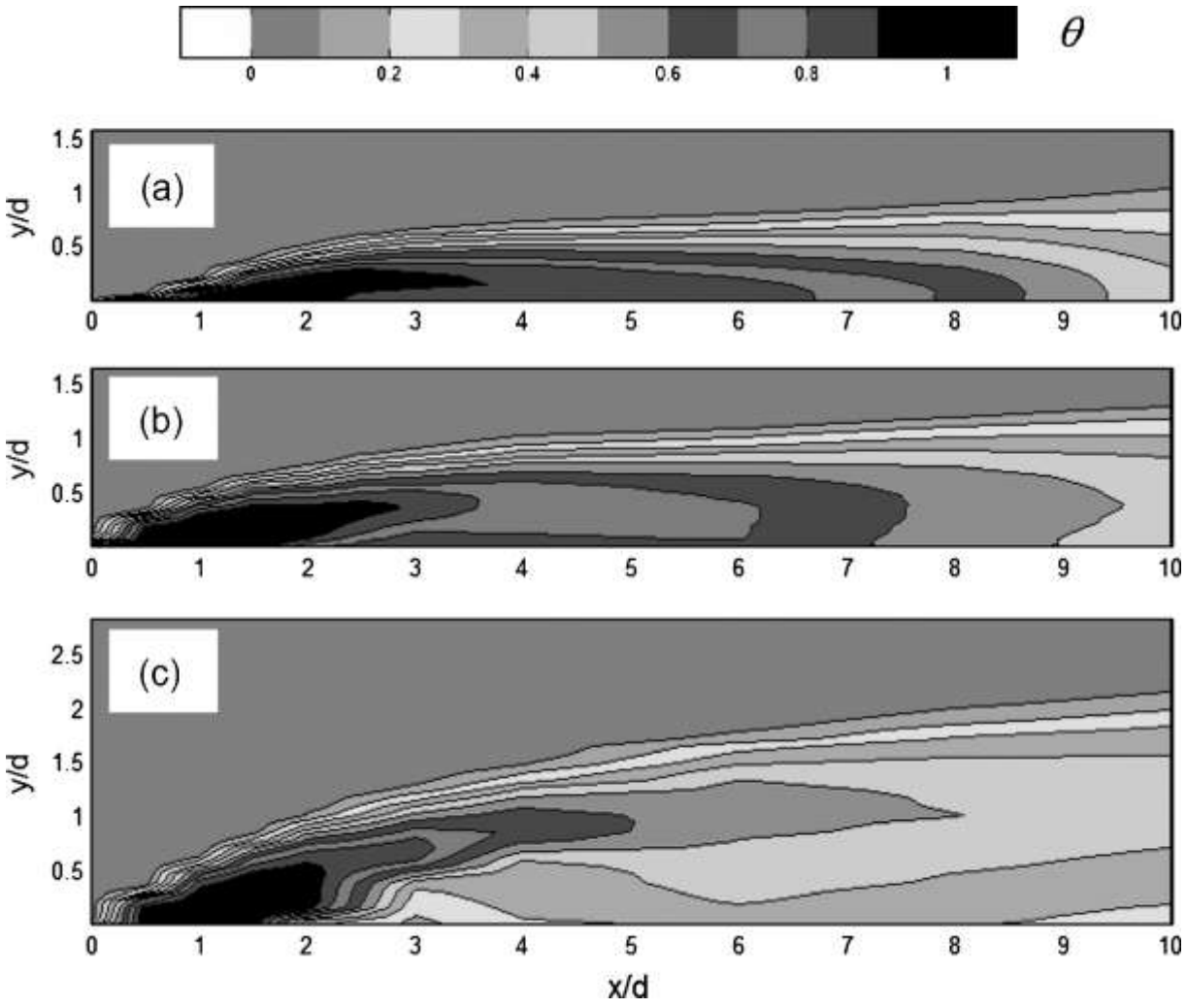

Figure 1 Thermal field profiles along centerline of coolant jets a) fully attached jet, b) detached and reattached jet, and c) fully detached jet taken from Bogard and Thole[1]

2.2 Measurement of effectiveness

Most of the studies and experiments are carried out for the holes drilled in the flat plate. The effectiveness calculation requires the measurement of the adiabatic wall temperature. The setup uses insulated test section of low conductivity to achieve nearly adiabatic surface. Goldstein et al.[2] measured the temperature using the array of thermocouples on an insulated test surface for cylindrical and shaped hole configuration. Thermocouple measurement is intrusive and can only gave data at particular point. The accurate surface temperature data can be collected by using infrared (IR) thermographic system. Gritsch et al.[3] and Peng and Jiang[4], used the thermocouple system along with IR to improve the accuracy of the measurement.

2.2.1 Experiment setup and similarities

There are several experiments conducted with the same coolant injection angle and similar flow parameters. The L/D ratio for the experiment was varied giving different results at the same location. Table 1 is reproduced from the paper Lutum and Johnson[5] summarizes the geometric and experimental boundary conditions for the different studies.

Table 1 Comparison of geometric and experimental conditions [5]

Geometrical Parameter					
Reference	Channel Width	Channel Height	Number of holes	P/D	L/D
	[mm]	[mm]	[-]	[-]	[-]
Goldstein et al.[2]	250	130	11	3	5.2
Pedersen et al.[6]	610	305	15	3	4
Sinha et al.[7]	610	610	7	3	1.75
Lutum and Johnson[5]	80	60	7	2.86	1.75-18
Fluid Boundary Condition					
Reference	Tu_∞	U_∞	D.R.	T_∞	T_c
	[%]	[m/s]	[-]	[°C]	[°C]
Goldstein et al.[2]	low	20-55	0.9	25	-
Pedersen et al.[6]	0.4	15-27	1.18	Heat-mass transfer analogy (section 2.2.2)	
Sinha et al.[7]	0.2	20	1.2	27	-23
Lutum and Johnson[5]	3.5	115	1.15	64	20

2.2.2 Heat-mass transfer analogy

The measurement of local effectiveness requires large-scale experiments to be performed with locally adiabatic walls. The heat flow from the wall has to be zero locally, for the effective measurement, which is difficult to achieve in the experiment. The difficulties involved with direct measurement of local temperature can be avoided by the heat-mass transfer analogy suggested by Pedersen et al.[6] . The foreign gas with the same temperature as the main flow is used to get density difference. The mass fraction 'c' of the foreign gas is related to adiabatic wall temperature giving similar formula as that of Eq.2.

$$\eta = \frac{c_\infty - c_{aw}}{c_\infty - c_{c.exit}} \qquad (6)$$

The indices of Eq.6 have the same meaning as the Eq.2. The analogy is valid for the case where Schmidt number, Sc for the mass transfer experiment is equal to the Prandtl number, Pr of the analogous heat transfer condition Pedersen et al.[6]. This method gives a more accurate measurement of the adiabatic wall temperature T_{aw}. The use of heat-mass transfer analogy was done by Johnson et al.[8] for measurement of the T_{aw} using the pressure sensitive paint (PSP) technique. Oxygen is used as a secondary gas. Concentration of the gas is related to the pressure measured by image intensity captured by CCD camera.

The PSP technique is more effective if the secondary gas has density close to the mainstream gas. However, in actual turbine, significant density difference is seen making the PSP measurement unreliable. N2 (ρ = 0.97) was used in some cases to study the effect of density ratio on the measurement data. Because the use of PSP to study film cooling effectiveness is a fairly new technique, comparison to similar studies was made by Johnson et al.[8] to validate its reliability as a measurement tool. For the comparison, a coolant stream of CO_2 (ρ = 1.53) is injected through a plate of the 5 cylindrical holes and a pitch P/D=3.This geometry and experimental parameters are chosen due to an abundance of data for similar cases in the open literature. The results matched closely with Lutum and Johnson[5] and several other literature cited by the author, proving the reliability and accuracy of the measurement technique.

2.3 Effect of parameters on centreline effectiveness

2.3.1 Variation of centreline effectiveness with X/D

As we go farther downstream, the coolant mixes with the mainstream and reduces the effectiveness of the cooling arrangement. It can be observed from Fig.2 that the centreline effectiveness of the film cooling goes on decreasing for the distance farther from the point of injection.

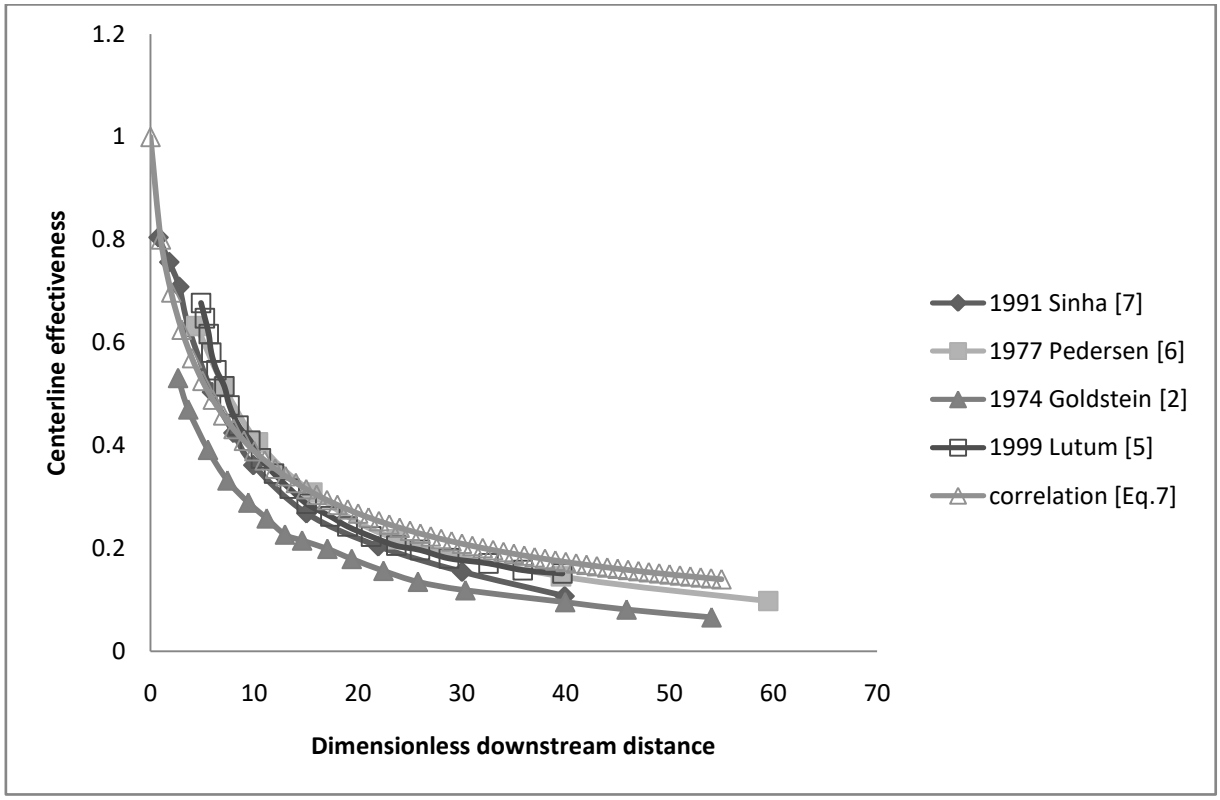

Figure 2 Comparison of centreline effectiveness for cylindrical holes for blowing ratio M = 0.5 and density ratio D.R ~ 1.0 reproduced from the respective papers.

Lutum and Johnson[5] have compared the results with Sinha et al.[7] and Goldstein et al.[2] and the results match closely for the same blowing and density ratios. The results are close enough for the blowing ratio of 0.2 to 2 and thus the correlation can be used for the general case. Pedersen et al.[6] mentioned such correlation given by the equation Eq.7 that best matches with their result. The equation gives the variation of centreline effectiveness η with dimensionless downstream distance ξ. The co-relation (Eq.7) thus can be used to validate the experimental results as it fits most of the data points plotted in Fig.2 with the exception of the Goldstein et al.[2]

$$\eta = \frac{1}{1 + 0.249\xi^{0.8}} \qquad (7)$$

2.3.2 Variation of centerline effectiveness with M.

It is observed from the Fig.3 and Fig.4 that the increase in mass flux ratio, M causes the increase in momentum flux ratio, I. For the same location of the airfoil, adiabatic effectiveness is lesser for the case with higher M.

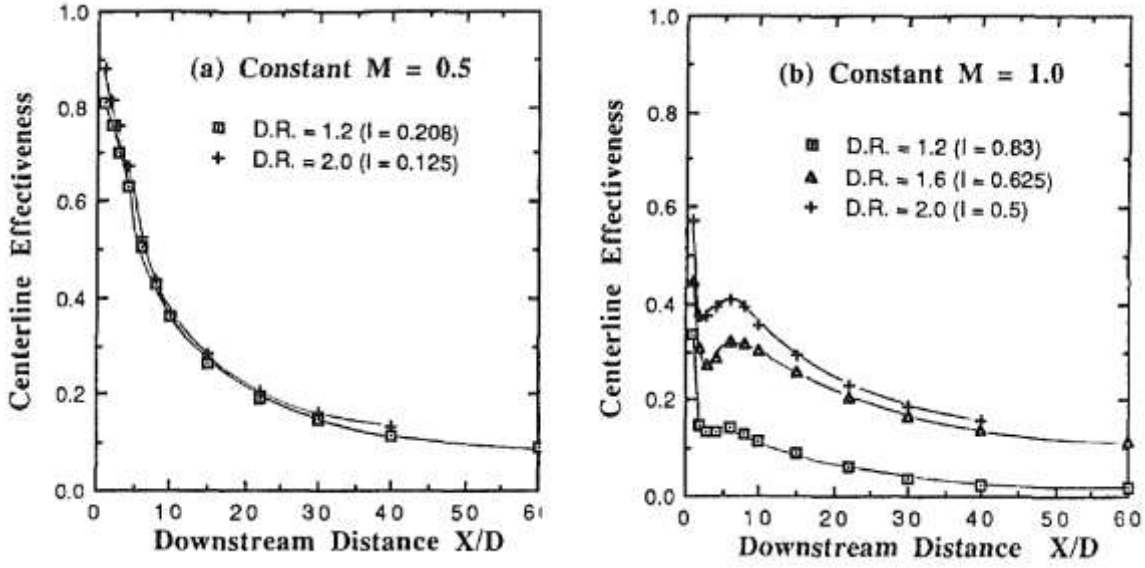

Figure 3 Comparison of centreline effectiveness along the dimensionless downstream distance for varying D.R and momentum flux ratio I. [7]

The sudden drop in the effectiveness can be seen in Fig.2b at the higher values of momentum flux ratio. Sinha et al.[7] explained the drop by attributing it to the detachment of the jet from the surface. The jet reattaches at some location along the downstream causing the rise in effectiveness. The reattachment of the jet can be explained by the loss in momentum along the flow causing the mainstream to push down the coolant jet. At a higher value of momentum flux I, the jet is detached permanently from the surface resulting in low values of η.

Pedersen et al.[6] performed the experiment for the hole with L/D = 40 compared to the L/D = 1.75 of Sinha et al.[7]. The shorter holes resulted in earlier detachment of the jet. The early detachment at smaller momentum flux ratio is due to the liftoff of the coolant because of the small effective injection angle reported by author [7]. Goldstein et al.[2] and Lutum and Johnson[5] reported a similar trend for different values of mass flux and momentum flux ratios. It can be observed from the Fig.3 and Fig.4 that the centreline effectiveness scales with the density ratio if it is less than one. For D.R higher than one, the centreline effectiveness is not affected as long as the jet is attached to the airfoil.

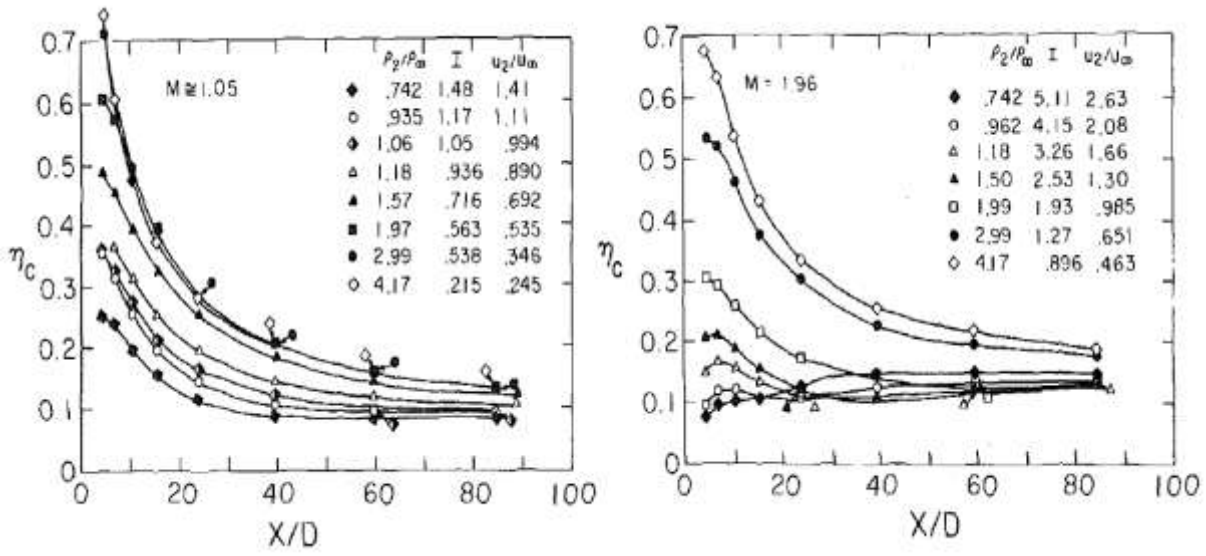

Figure 4 Comparison of centreline effectiveness along the dimensionless downstream distance for varying D.R and momentum flux ratio I. [6]

2.4 Lateral effectiveness variation

The ejected coolant jet spreads across the span of the airfoil. Along the span, due to mixing with mainstream and the vortex formation, jet may or may not remain attached to the surface. Fig.5 gives the comparison of the results performed by the Goldstein et al.[2] and Sinha et al.[7] for half pitch distance and downstream distance X/D ~ 7. Sinha et al.[7] have given the local effectiveness data for X/D of 1, 10 and 15. The data is interpolated to get the effectiveness value at X/D = 7. The results match for the same X/D and blowing ratio.

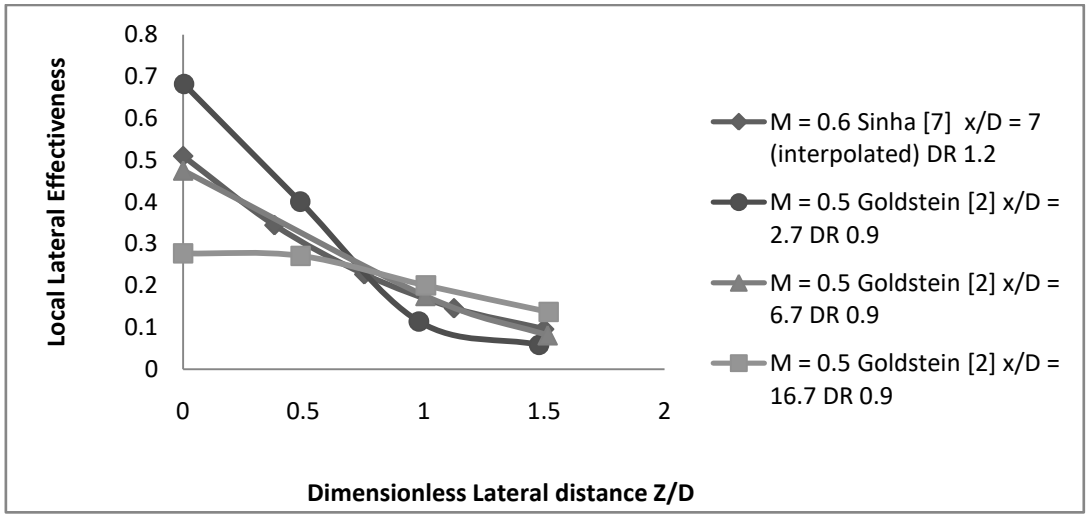

Figure 5 Comparison of local lateral effectiveness η_L for cylindrical holes for blowing ratio M ~ 0.5 and density ratio D.R ~ 1.0 reproduced from Sinha et al.[7] and Goldstein et al.[2]

The lateral effectiveness η_L just at the beginning of the airfoil is highest and goes on decreasing as the downstream distance is increased. The lateral effectiveness attains the constant value at a distance farther from the start of the airfoil. This is because of the various factors like increased turbulence, the formation of eddies and mixing with the mainstream gas. The η_L value is dependent on the momentum flux ratio.

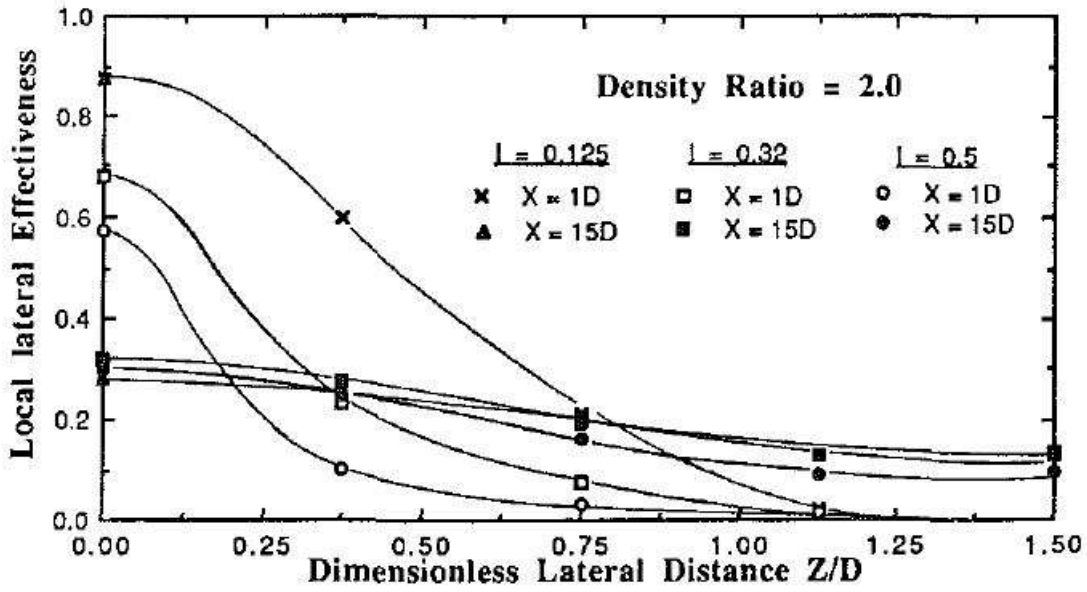

Figure 6 Local lateral effectiveness distribution at two different streamwise location (X/D =1 and X/D =15) for D.R. = 2 [7]

Sinha et al.[7] presented the result indicating the decrease in lateral effectiveness with an increase in the momentum flux ratio. Results of Fig.6 are noteworthy as the variation of η_L along the length and with the momentum flux can be observed. As momentum flux is increased coolant gas is more likely to lose contact with the airfoil. Thus the mainstream gas enters the space where coolant gas is detached from the surface and reduces the effectiveness of the cooling arrangement.

Chapter 3

EFFECT OF HOLE GEOMETRY AND CONFIGURATION ON FILM COOLING

3.1 Introduction

The manufacturing methods like laser drilling or electrodischarge machining (EDM) are used for placing the holes on the surface of the airfoil. The drilling of holes should increase the effectiveness of the cooling arrangement, as it requires expensive manufacturing techniques. Cylindrical holes are easy to drill on the airfoil but provide a limited increase in the effectiveness of the film cooling. Thus, it is important to study the effect of the geometry parameters to improve the performance of the cylindrical holes. Discussion for the configurations like fan-shaped and trenched holes are made later in the report.

3.2 Fan-shaped holes

Fan shaped holes are more efficient than cylindrical holes as they have the area expanding in the lateral direction which slows down the coolant jet and keeps it closer to the airfoil surface. The manufacturing of the fan-shaped geometry is difficult and expensive. Fig 7 is the schematic diagram for fan shaped holes.

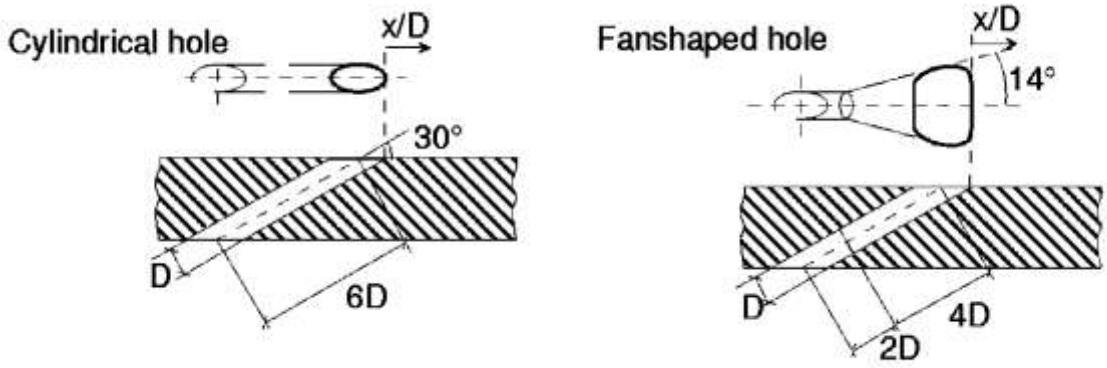

Figure 7 Hole configuration tested by Saumweber et al.[9]

Saumweber et al.[9] analysed the cylindrical and fan-shaped hole shown in Fig.6 for comparison of the performance. The similar studies were performed by Gritsch et al.[3] where they investigated the effects of the hole geometry like the compound angle, area ratio, P/D ratio on the effectiveness with the fan-shaped hole configuration.

3.2.1 Laterally averaged effectiveness comparison

Lutum et al.[10] have studied cylindrical and the fan-shaped holes for varying momentum flux ratio. The results are presented in in Fig.9 for laterally averaged effectiveness versus the dimensionless downstream distance S/D (or X/D). Lutum et al.[10] have compared different arrangements of cylindrical holes. Configuration one and two are the cylindrical configuration with different pitch to diameter ratio. This will help in deciding how close the holes should be drilled on the airfoil so that the optimum results are obtained. Configuration three has the compound angle of 60˚ relative to the mainstream flow direction. The configuration four is fanshaped and five is laidback fan geometry. Saumweber et al.[9] reported slight increase in the effectiveness for the laidback fan configuration thus it is not studied. The details of the configuration can be found in Fig.8.

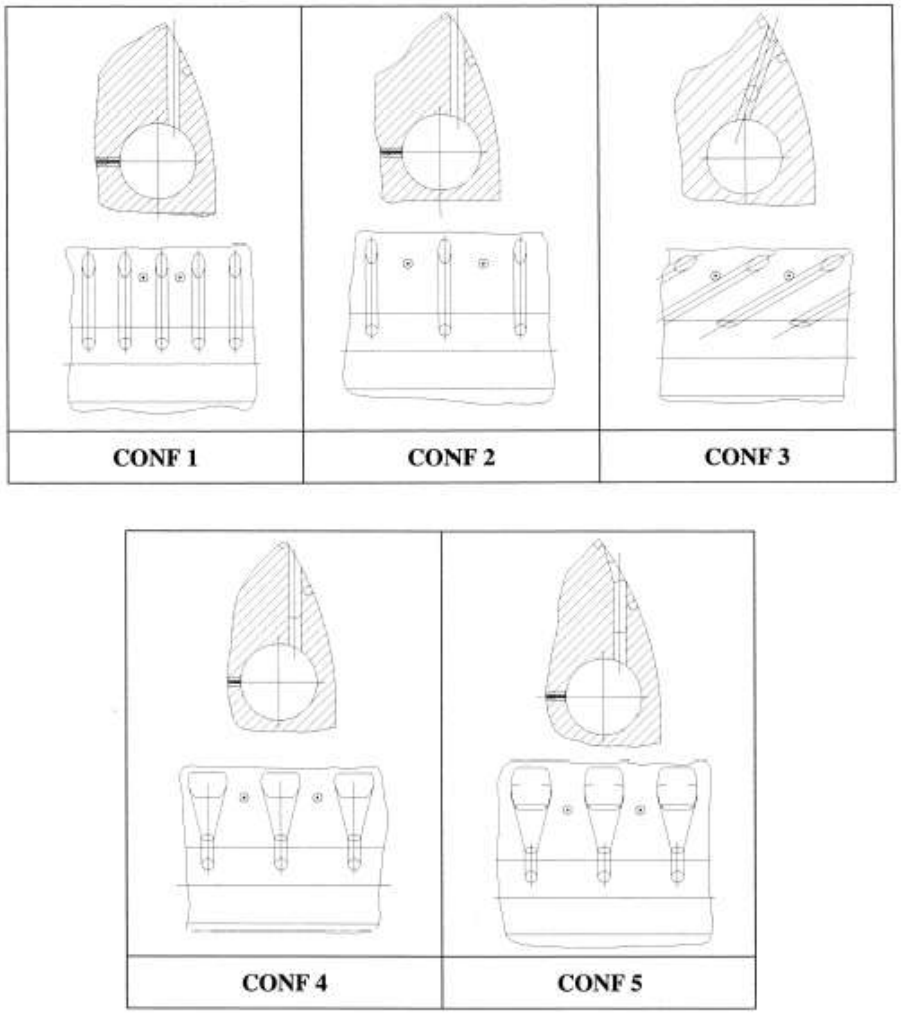

Figure 8 Film cooling geometry studied by Lutum et al.[10]

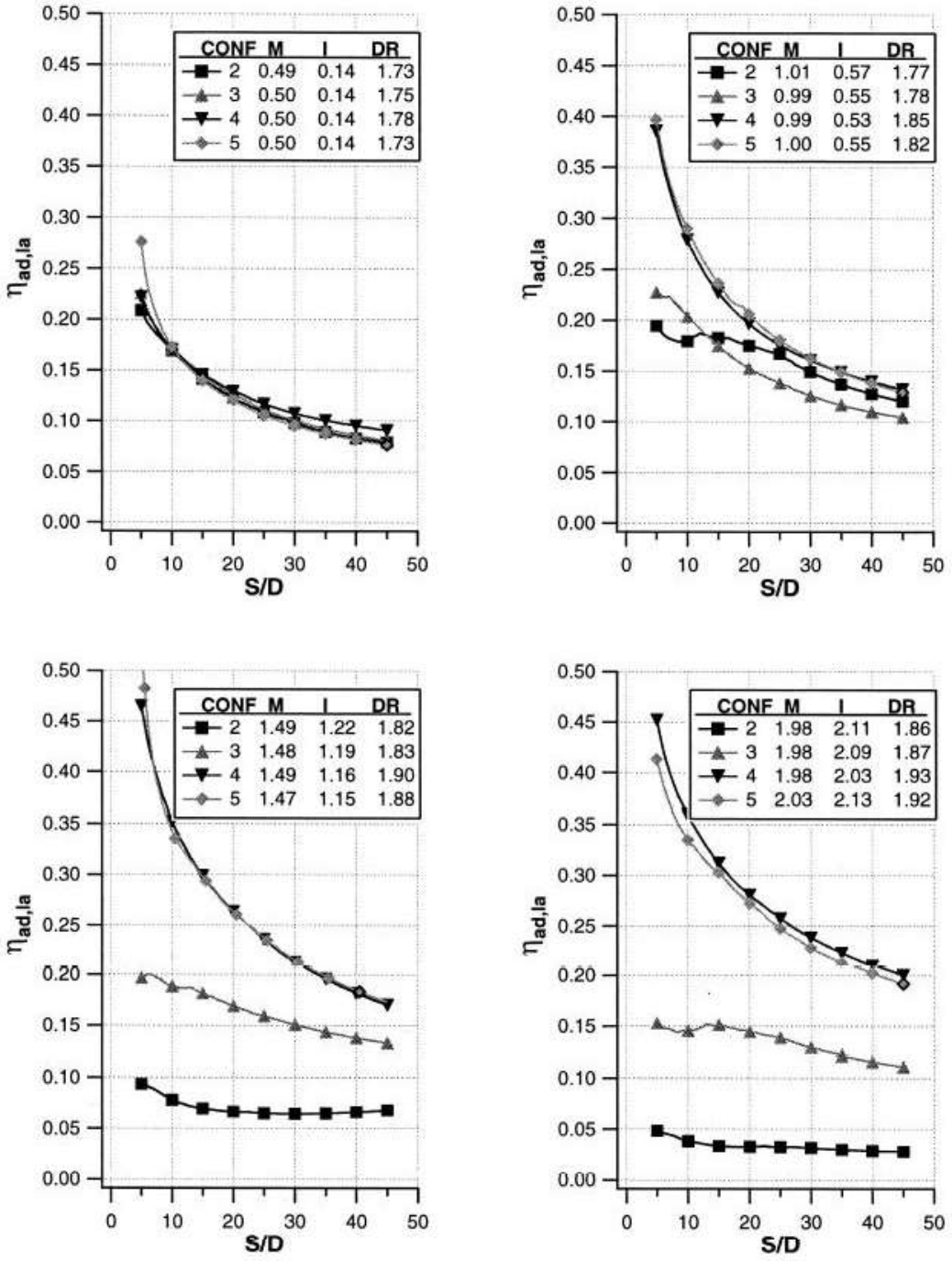

Figure 9 Comparison of laterally averaged film cooling effectiveness for CO_2 injection versus downstream distance. [11]

For smaller momentum flux ratio, the behaviour of all the configurations is identical. As the value of I increases, the effectiveness $\overline{\eta_L}$ is higher for the fan-shaped configuration. It can be concluded from the data that the use of fan-shaped holes is justified for the mass flux ratio greater than 0.5 as effectiveness is much higher than the cylindrical holes. As blowing ratio is

increased to two, fan shaped holes continue to perform better. The increase in $\overline{\eta_L}$ is because of the decreased momentum due to the widening of the holes at the exit. The widening also helps in effective spreading of the coolant in the lateral direction. For the compound hole configuration 3, the effectiveness is lesser than the fan-shaped holes but greater than the cylindrical holes with 0 degree compound angle. The compound angle helps to increase effectiveness as the inertia of coolant in flow direction is reduced. The separation of jet is still observed for configuration 3 because of the cylindrical geometry. Gritsch et al.[3] studied the effect of the compound angle for fan-shaped holes and the results for laterally averaged effectivenss are given in Fig. 13b. The increase in compound angle increased the effectiveness. As fan-shaped configuration is used, small change in the blowing ratio did not have significant effect on the effectiveness. The laidback fan configuration does not give notable increase in the effectiveness. Saumweber et al.[9] reported the similar trend of laterally averaged effectiveness for various values of turbulent intensities TU and L/D ratio.

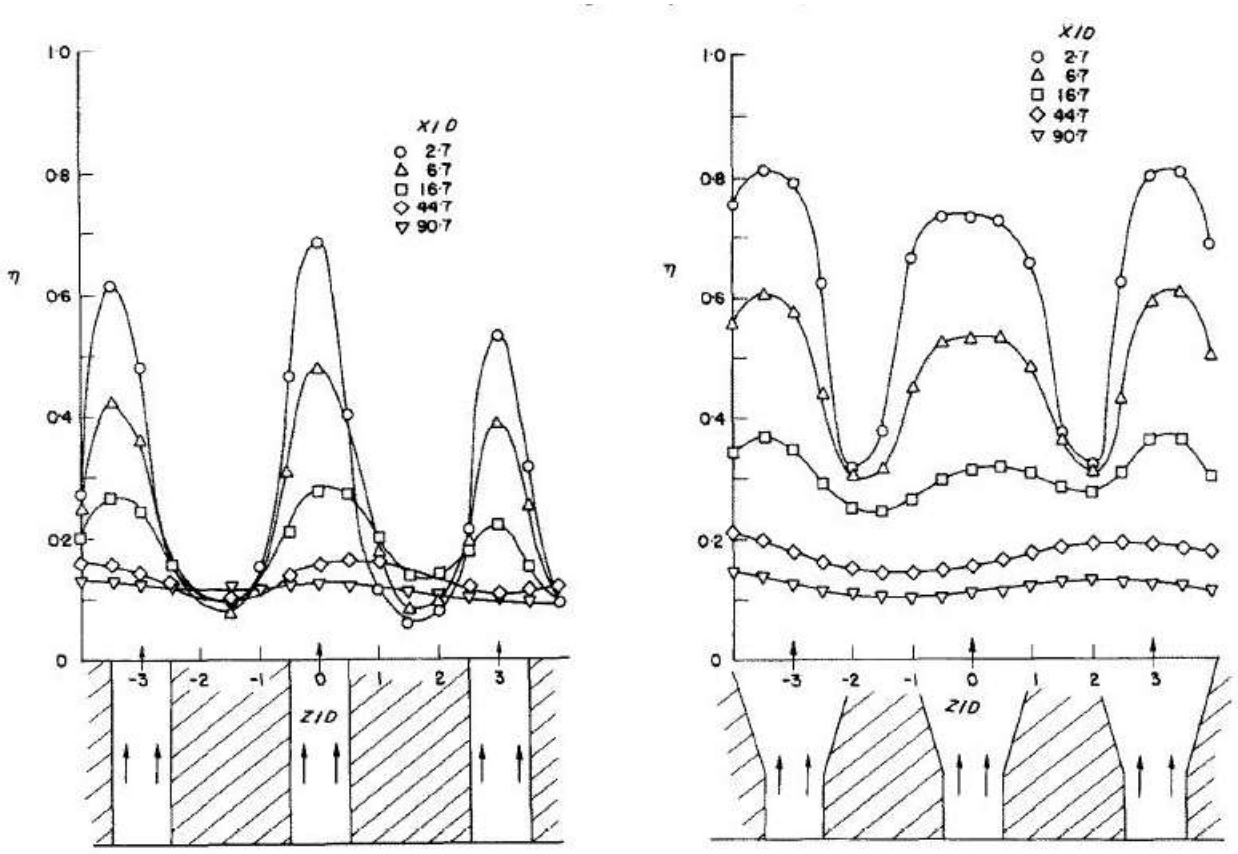

Figure 10 Lateral variation of film cooling effectiveness for P/D = 3 and M = 0.5 at different downstream location for the (a) Cylindrical holes (b) Shaped holes [2]

3.2.2 Local lateral effectiveness comparison

Goldstein et al.[2] performed the experiment for the shaped hole with 10˚ side angle of the fan and presented the distribution of local lateral effectiveness for the range of X/D values. Effectiveness peaks at the point of injection and at larger X/D location, the lateral variations are smoothed out. From Fig.10 it can be observed that fan shaped holes give better lateral spreading of the coolant and thus the better effectiveness than the cylindrical holes. The Fig.10 can also used to decide how close the holes are to be placed on the airfoil.

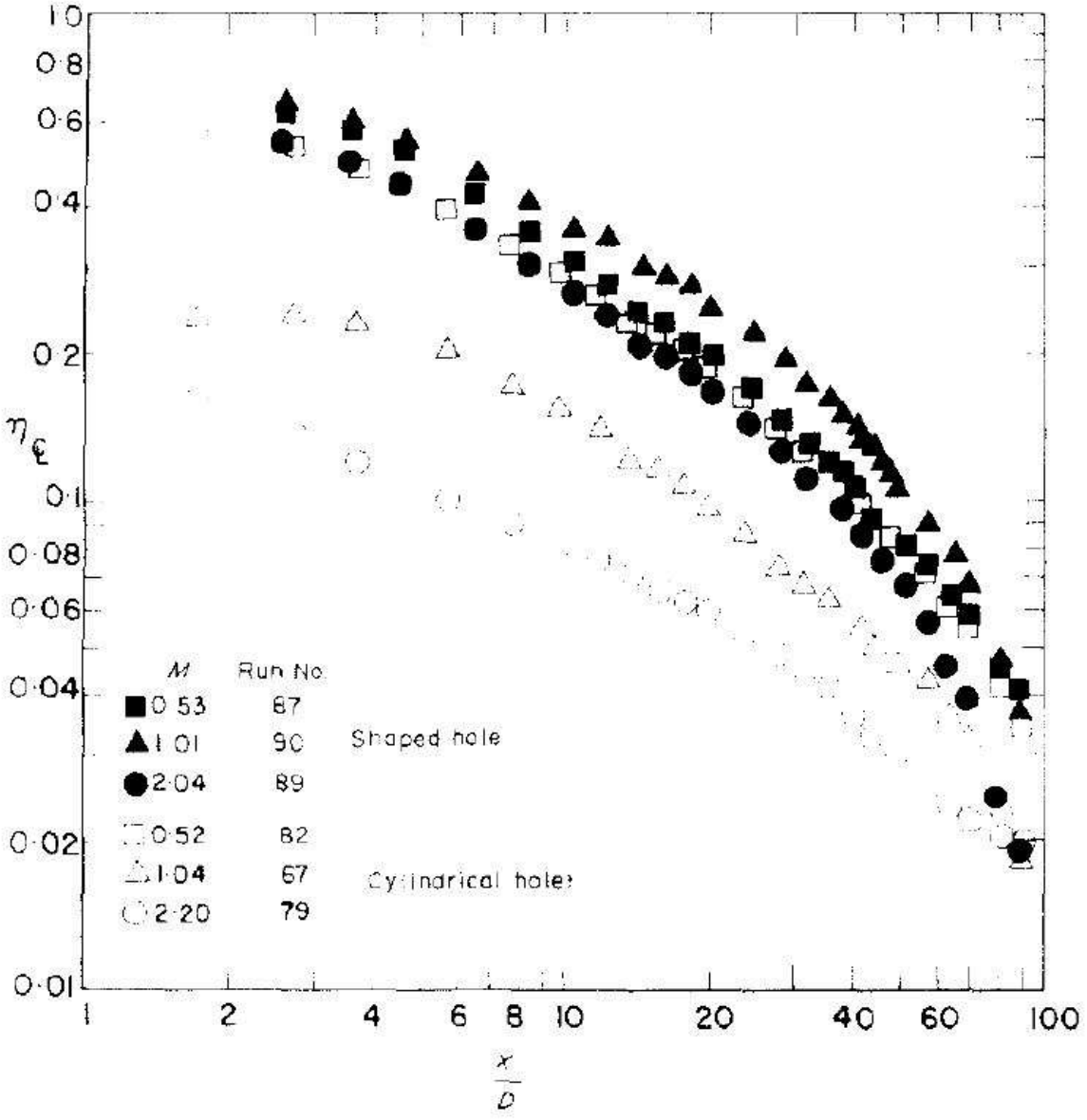

Figure 11 Centerline film cooling effectiveness for different blowing ratios and single hole injection for the (a) Cylindrical holes (b) Shaped holes [2]

3.2.3 Centerline effectiveness comparison at different blowing rates

Fig.10 gives the centreline effectiveness variation for the cylindrical and fan-shaped hole configuration for different blowing rates. It can be observed that for the blowing rate greater than one, the fan-shaped holes are more effective for cooling of the airfoil. Unlike cylindrical holes, the value of centreline effectiveness for fan-shaped holes increases when blowing ratio increases from 0.5 to 1.The increase in effectiveness is because of the expanded exit of the fan-shaped holes decreasing the exit velocity and thus keeping the jet closer to the surface of the airfoil. Peng and Jiang[4] reported a similar trend for the blowing ratio ranging from 0.5 to 1.5 and can be observed in Fig 12

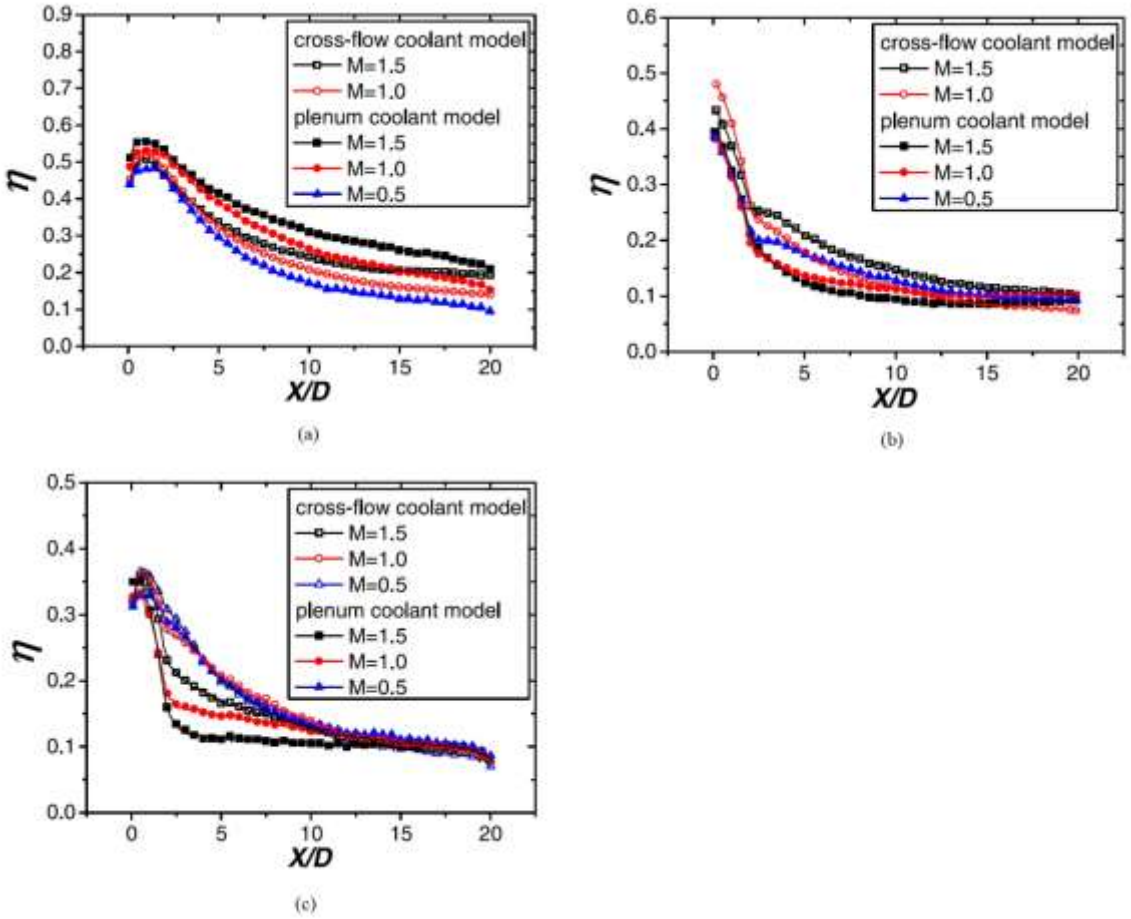

Figure 12 Variation of laterally averaged effectiveness for (a) Shaped holes (b) Trenched holes (c) Cylindrical Holes [3]

3.3 Effect of hole geometry

The assessment of the geometrical quantities is important to avoid the manufacturing uncertainties and to have better control over the cooling system. The study of some of the parameters like pitch to diameter ratio and effect on compound angle on the performance of the film cooling was carried out by Gritsch et al.[3]. Some of the investigated parameters like length to diameter ratio and hole exit to inlet area ratio (for cylindrical holes with manufacturing error) had little effect on the performance of film cooling.

3.3.1 Effect of pitch to diameter ratio

The P/D ratio affects the lateral effectiveness of the film cooling arrangement as it decides the effective spreading of the coolant gas and how close the holes can be placed. Fig 13a represents the increase in effectiveness with the increase in P/D. For smaller P/D ratio, the coolant does not spread properly as the holes are too close to each other. For larger P/D ratio, mainstream gas mixes with coolant thus reducing the overall effectiveness of the film cooling. Thus, it is essential to get the optimum value of the P/D ratio for better performance.

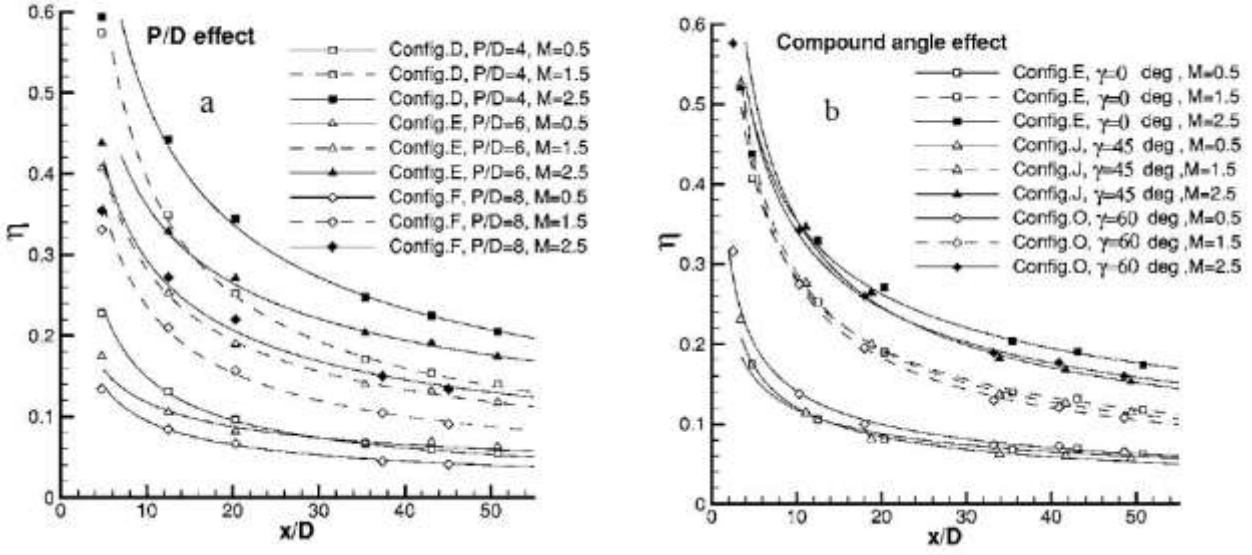

Figure 13 Effect of geometry parameters on the laterally averaged film cooling effectiveness for different blowing ratios for the fan-shaped holes [2]

Chapter 4
FILM COOLING PREDICTION

4.1 Introduction

The experimental approach involves drilling the holes on the surface of the airfoil and carrying out the tests for understanding of the physical mechanism involved in film cooling flow-fields. Computational fluid dynamics is effective, fast and accurate in predicting the data thus increasing the reliability of the design.

4.2 Mathematical modelling

Direct numeric simulation (DNS) and large eddy simulation (LES) use a lot of computing power although they give refined results. One can get accurate results by using time-averaged continuity, momentum, and energy equation for the statistically steady, incompressible, and turbulent flow. Equation 8, 9 and 10 are time averaged continuity, momentum, and energy equation and U, T, P are average velocity components, temperature and pressure. The terms u', T' are the fluctuating velocity and temperature components, respectively.

Continuity Equation

$$\frac{\partial U_i}{\partial x_i} = 0 \qquad (8)$$

Momentum Equation

$$\rho U_j \frac{\partial U_i}{\partial x_j} = -\frac{\partial P}{\partial x_j} + \frac{\partial}{\partial x_j}\left[\mu\left(\frac{\partial U_i}{\partial x_j} + \frac{\partial U_j}{\partial x_i}\right) - \rho\overline{u_i' u'}_j\right] \qquad (9)$$

Energy Equation

$$\rho U_j \frac{\partial T}{\partial x_j} = \frac{\partial}{\partial x_j}\left[\frac{\mu}{\mathrm{Pr}}\left(\frac{\partial T}{\partial x_j}\right) - \rho\overline{T' u_j'}\right] \qquad (10)$$

4.3 Turbulence model

The equation 9 is called the Reynolds-averaged Navier-Stokes (RANS) equation. The term $\rho\overline{u_i'u_j'}$ in RANS is known as Reynolds stress R_{ij} . RANS equations are closed by modelling of the term R_{ij} as a function of mean flow thus removing the fluctuating components of the velocity. In 1877 Boussinesq introduced the concept of eddy viscosity for solving the closure problem.

Common models

1. K-ε model
2. K-ω model
3. SST (Menter's shear stress transport)
4. RSM (Reynolds stress equation model)
5. RNG (renormalization group)

4.4 Details of flow in film hole

Leylek and Zerkle[11] documented the flow in film cooling hole for blowing ratio M=0.5 and M=2 and can be seen in Fig.14.

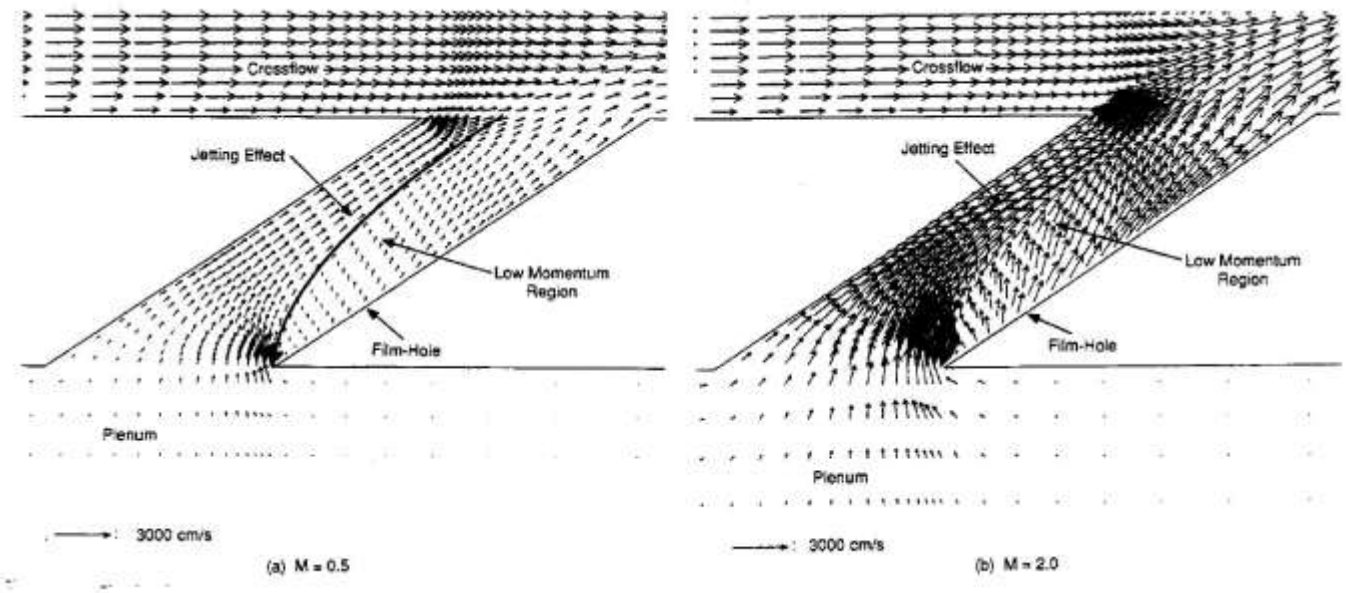

Figure 14 Computed velocity vectors on centerline plane of film hole [11]

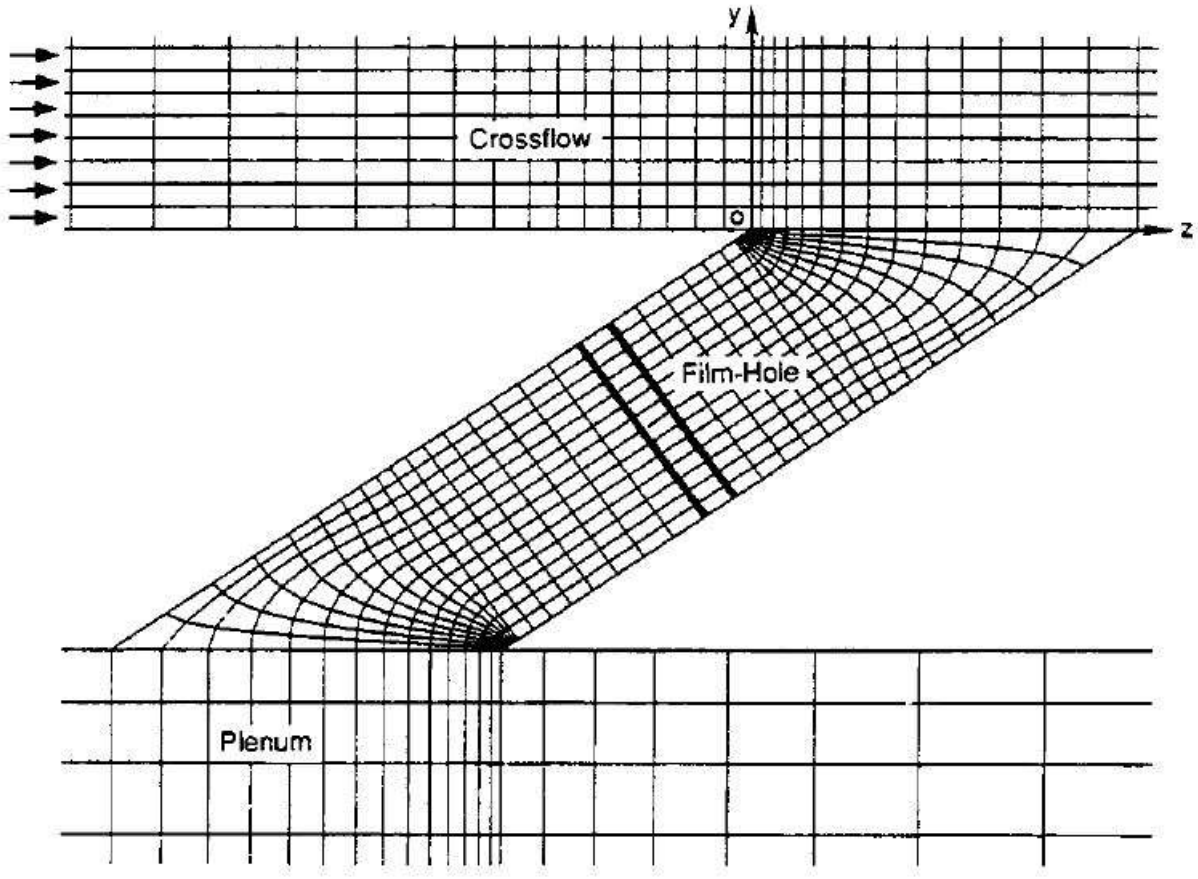

Figure 15 Computational gird for the cylindrical film hole [13]

The jetting effect is observed in the film cooling hole (refer Fig.14). The flow is not fully developed in the pipe as L/D ratio is low. The jetting effect increases with the increase in the blowing ratio. The jetting effect may be explained by the counter-rotating vortex of Fig.16 which is created at the hole inlet when flow in the plenum touches the sidewalls of the hole. Fig.15 shows the cross-section of the pipe where the velocity vectors are computed for studying the counter-rotating velocity vectors of Fig.16. The jetting effect increases with the increase in blowing ratio thus resulting in turbulent mixing of mainstream and coolant jet because the effect pushes the coolant jet away from the surface. The mainstream gas enters underneath the coolant jet and reduces the effectiveness of the cooling arrangement. This vortex in the hole continues to grow downstream of the flow causing the jet to lift from the airfoil surface. This reduces the effectiveness and increases the heat transfer to the airfoil. CFD papers report the two dimensional plot of the vortex structure on a plane perpendicular to the airfoil (Refer mutually induced velocity plane of Fig.17).The vortex structure forms shape of kidney and thus called as kidney vortex.

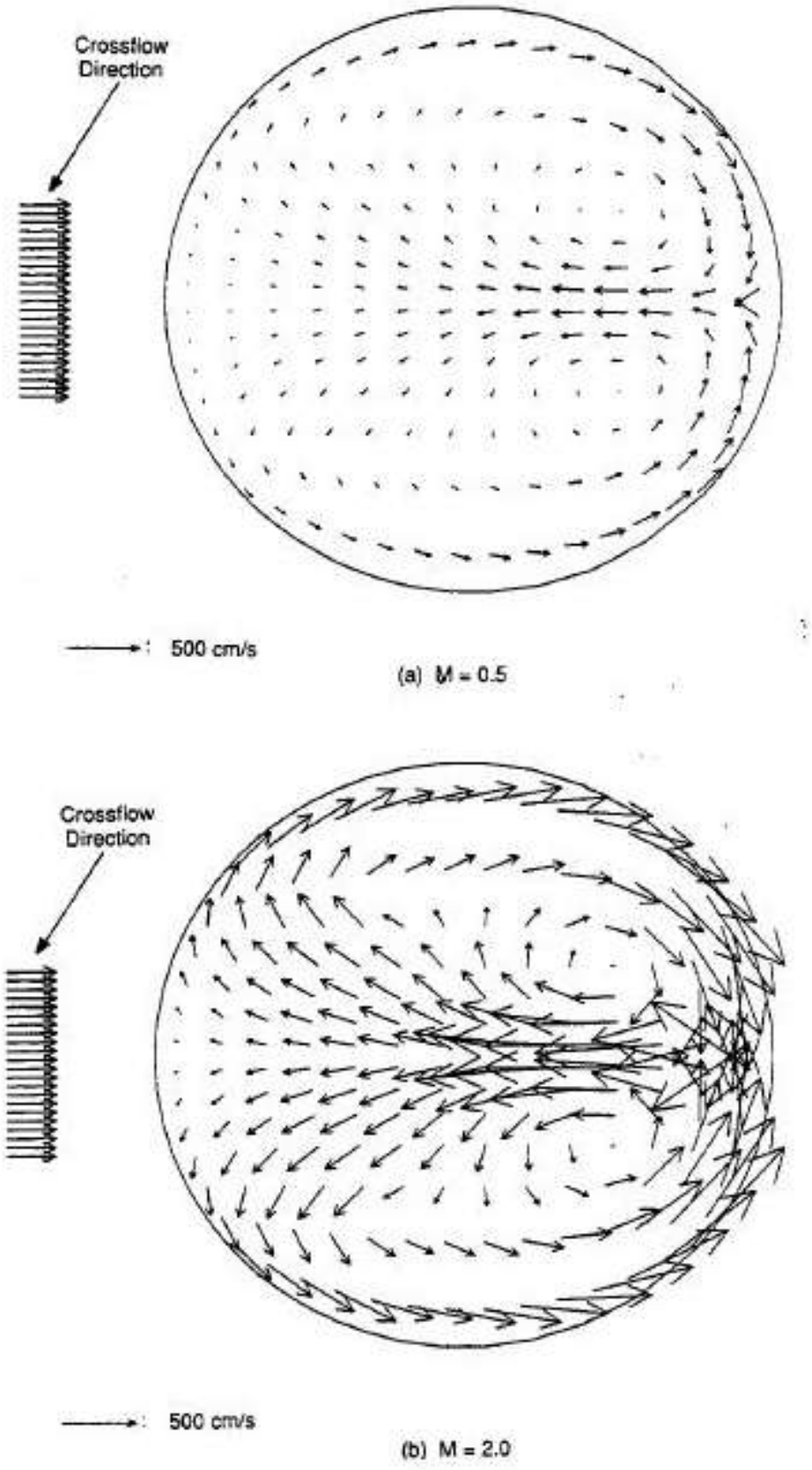

Figure 16 Counter rotating vortex velocity vectors at plane perpendicular to flow direction [13]

4.5 Kidney vortex in cross-flow jet

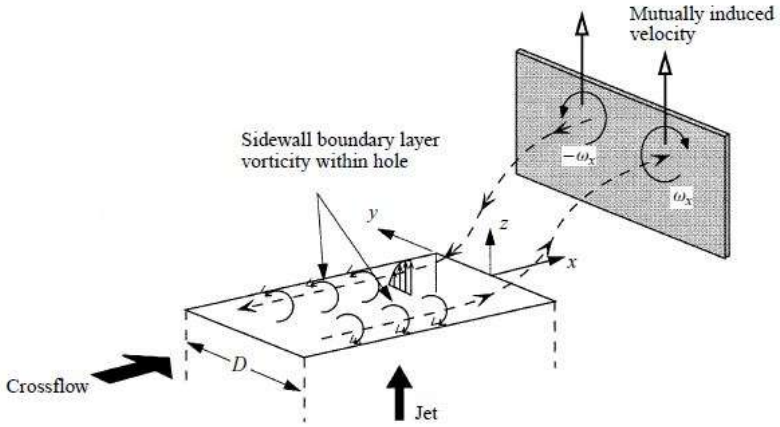

Figure 17 Kidney vortices due to hole side wall vorticity. [14]

Haven and Kurosaka[12] performed water tunnel experiments to study the effect of hole geometry on the crossflow jet. They used laser-induced fluorescence (LIF) and particle image velocimetry (PIV) for visualization of the data. The kidney vortex is formed due to the sidewall boundary layer of the hole generating the vorticity along the stream direction. The schematic of the flow can be noted from Fig.17. The dotted arrows represent the vortex sheet travelling in the crossflow direction. The vortex formed in the hole exits and continues to grow if hole has smaller dimension in the lateral direction. The images of Fig. 18 are capured right after the coolant leaves the hole. The kidney vortices when brought closer together increase by the mutual induction of velocities. The growth of vortex causes the separation of the coolant jet which reduces the lateral effectiveness of the cooling arrangement. The LIF images of Fig.18 show the liftoff of the coolant gas in the vertical direction. It can be noted that the holes with larger lateral dimension have less effect of the kidney vortex. Leylek and Zerkle[11] plotted the counter-rotating and kidney vortex at dimensionless downstream location X/D = 5 as can be seen in Fig.19. It can be confirmed that the flow tends to move in vertical direction with respect to the airfoil as the blowing ratio is increased. Thus it is important to minimize the formation of vortices right from the coolant hole to get better results from the geometry.

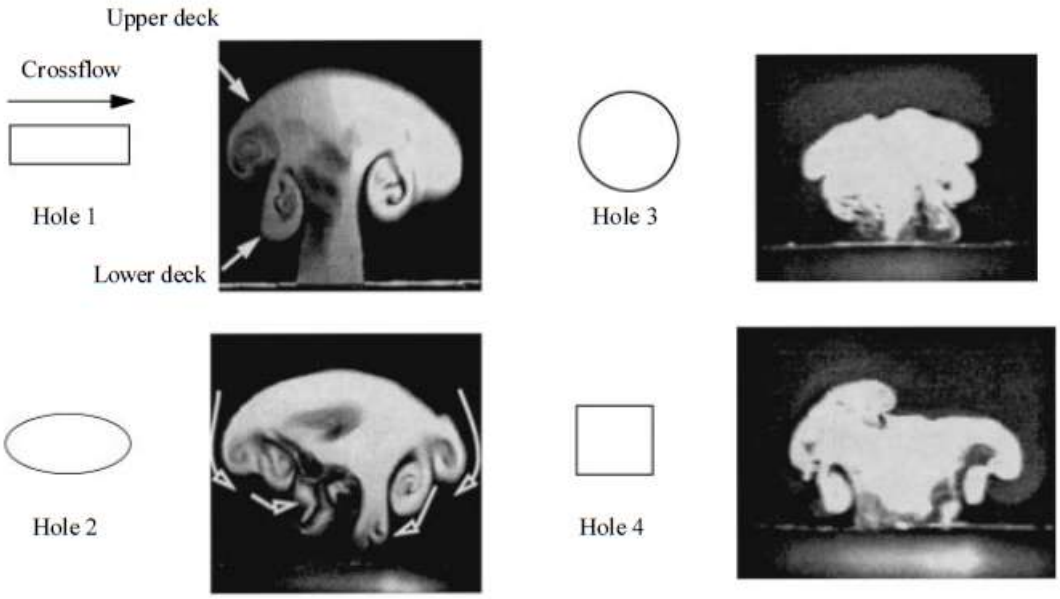

Figure 18 Laser induced fluorescence (LIF) of kidney vortex for different hole geometries at velocity ratio 1.6. [14]

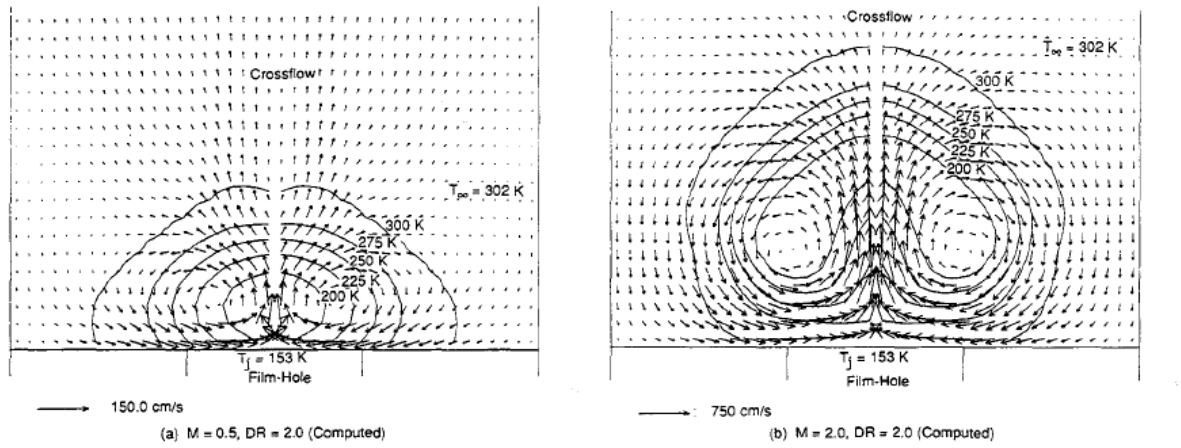

Figure 19 Kidney shaped cross-section of coolant jet for blowing ratio (a) M = 0.5, D.R. = 2 (b) M = 0.5, D.R =2 at X/D = 5. [13]

Chapter 5
FILM COOLING USING TRENCHED HOLES

5.1 Introduction

The manufacturing cost for the shaped hole is higher compared to the straight hole. The trenching of the cylindrical hole is done because it can reduce the cost and can give the comparable results to that of the shaped holes.

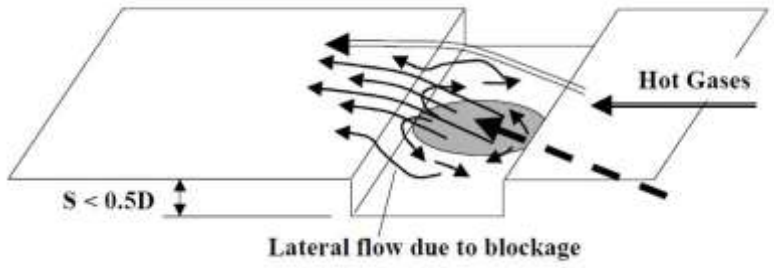

Figure 20 Trenched hole configuration studied by Bunker. [15]

Bunker[13] investigated the use of discrete film holes to feed a continuous surface slot. The configuration studied by the author is shown in Fig.20, and it is called as trenched hole.

5.2 Effect of trench geometry

For the trenched hole geometry, the slots are machined on the surface of the airfoil which can weaken the structure because of the thermal stresses. It is desirable to have less depth for the trench with higher effectiveness than the cylindrical hole case. Thus the variation of effectiveness with hole geometry is to be studied for choosing optimum hole geometry which can give highest effectiveness.

5.2.1 Effect of depth of the trench

Bunker[13] tested the two cases of the holes in the experiment namely axial film holes and the other with the same holes inside a shallow trench. The trench hole is called as shallow trench if the depth is less than the film hole throat diameter. The hole has inclination angle of 30-degrees, pitch to diameter ratio of 3.57, and length to diameter ratio of 5.7.

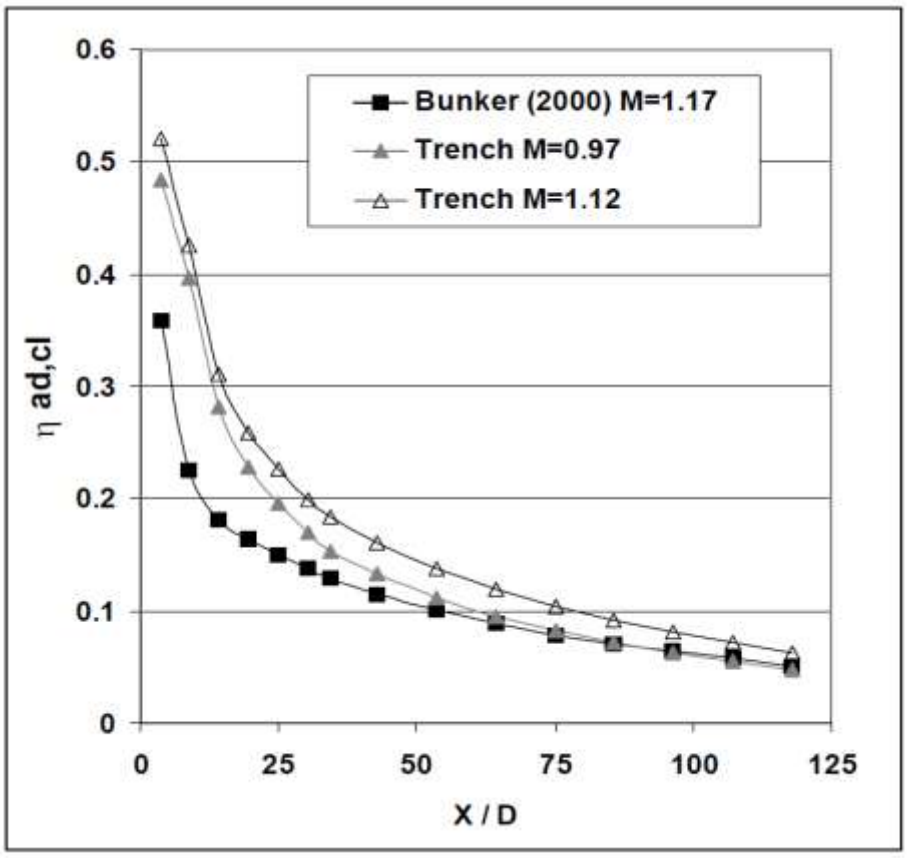

Figure 21 Centerline adiabatic effectiveness for the shallow trench geometry [13]

The adiabatic film effectiveness for the shallow trench geometry is shown in Fig. 21 for blowing ratios around M=1. In comparison to the conventional axial film holes, the trench geometry provides improved performance over most of the downstream surface, with the greatest improvement of about 50 to 75% in the near-hole region of x/D < 40. The increment in effectiveness is comparable to that of the shaped holes and certainly greater than the cylindrical holes.

The mechanism for this improved film performance can be explained by Fig.20. The trench forms a sub-surface which protects the film hole exit from the immediate intrusion or interaction with the hot gases. Thus, it is important that the upstream edge of the trench be close to the edge of the film hole exit. The downstream edge of the trench acts as a blockage element to the ejected coolant, which forces a portion of the cooling air to spread laterally within the trench prior to issuing onto the upper surface. This blockage reduces or disturbs the vortex motion of the cooling jets, such that hot gases are not pulled under the cooling air.

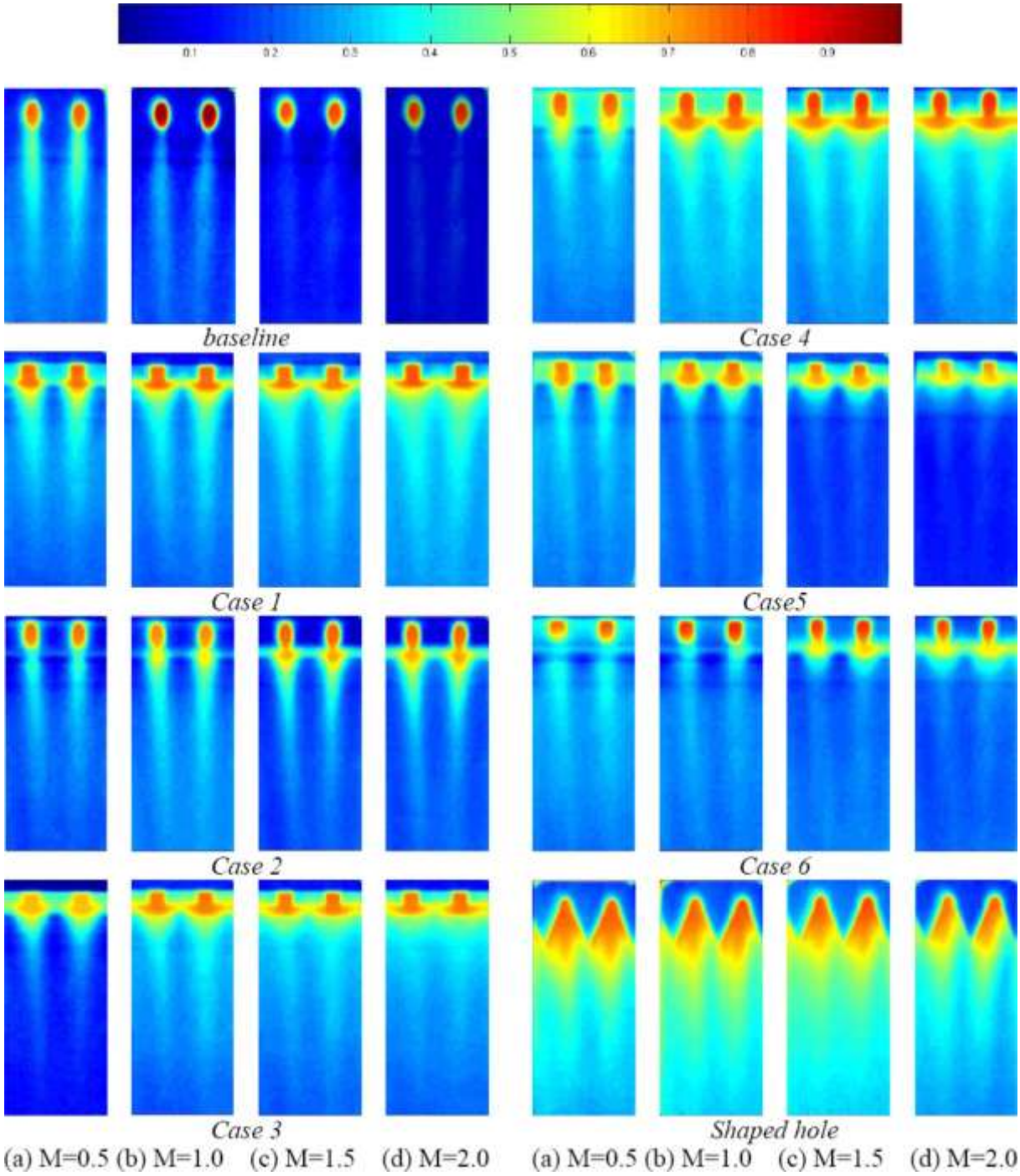

Figure 22 Centerline effectiveness for different cases tested by Lu et al.[14]

Lu et al.[14] studied the effect of trenched depth and width of the trench on on the film cooling effectiveness. The geometry variations tested by Lu et al.[14] are given in Table.2. The blowing ratio has a significant effect on the performance of the film cooling with trenched hole configuration. The increase in the blowing ratio increases the centreline

effectiveness for the case of the trenched hole as observed in Fig.22. The increase is because of the downstream edge acting as a barrier thus not allowing the flow to separate from the surface. Lu et al.[14] reported an optimum value of depth to diameter ratio 0.75 for the hole for which the inclination angle is 30 degree and L/D is two. From basic trigonometry one can say that the depth for 30 degree should be greater than 0.577D for complete blockage of the coolant gas. Increasing the depth beyond the optimum value reduces the effectiveness.[13] This is because the mainstream gas enters in the trench and mixes with coolant. For shallow trench, most of the depth is occupied by the coolant gas thus giving higher value of the effectiveness.

Table 2 Film hole and flow geometry

Case Number	Width of the trench	Depth of the trench
Case 1	2 D	0.5 D
Case 2	3 D	0.5 D
Case 3	2 D	0.75 D
Case 4	3 D	0.75 D
Case 5	2 D	1 D
Case 6	3 D	1 D

Low depth for trenched holes is more effective and can be observed from Fig.21. For case 5 and 6 which has the highest depth amongst the geometries Lu et al.[14] studied, the effectiveness value is less than the shallow holes.

5.2.2 Effect of width of the trench

The trenched hole with width greater than the hole diameter is called as wide trenched hole. Waye and Bogard[15] have studied different configurations of the trench shown in Fig.23. The highest effectiveness is obtained for the configuration 2. The results of configuration 3 are very much similar to the configuration 2. The presence of rectangular block upstream of the hole prevented the mainstream gas entering into the trench thus increasing the film effectiveness in configuration 2.

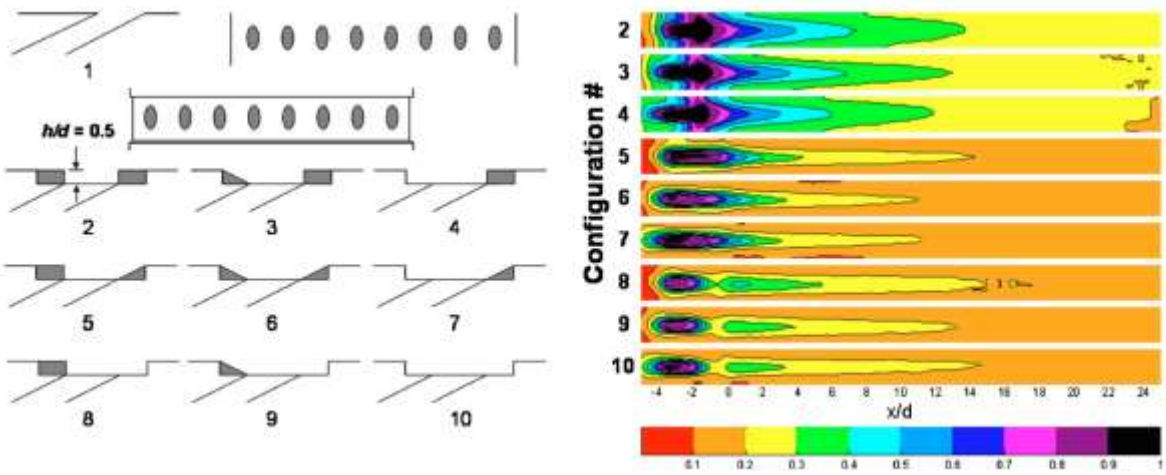

Figure 23 Spatial plots of lateral effectiveness for different configurations [15]

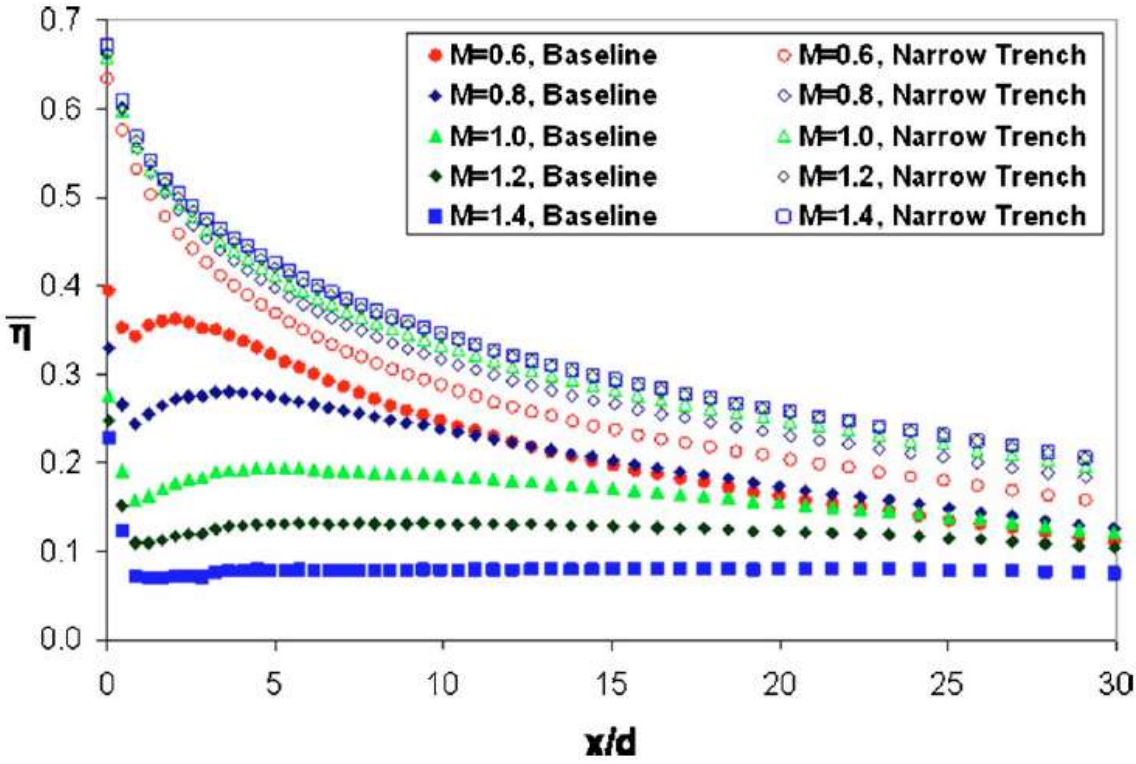

Figure 24 Comparison of the laterally averaged adiabatic effectiveness for narrow trench and axial cylindrical holes. [15]

For the same downstream location, narrow trench is better than the wide trench as can be compared from Fig.24 and Fig.25. Narrow trench performs better than all other configurations because the coolant gas does separate from the surface and spreads in lateral direction and can be observed in Fig.26.

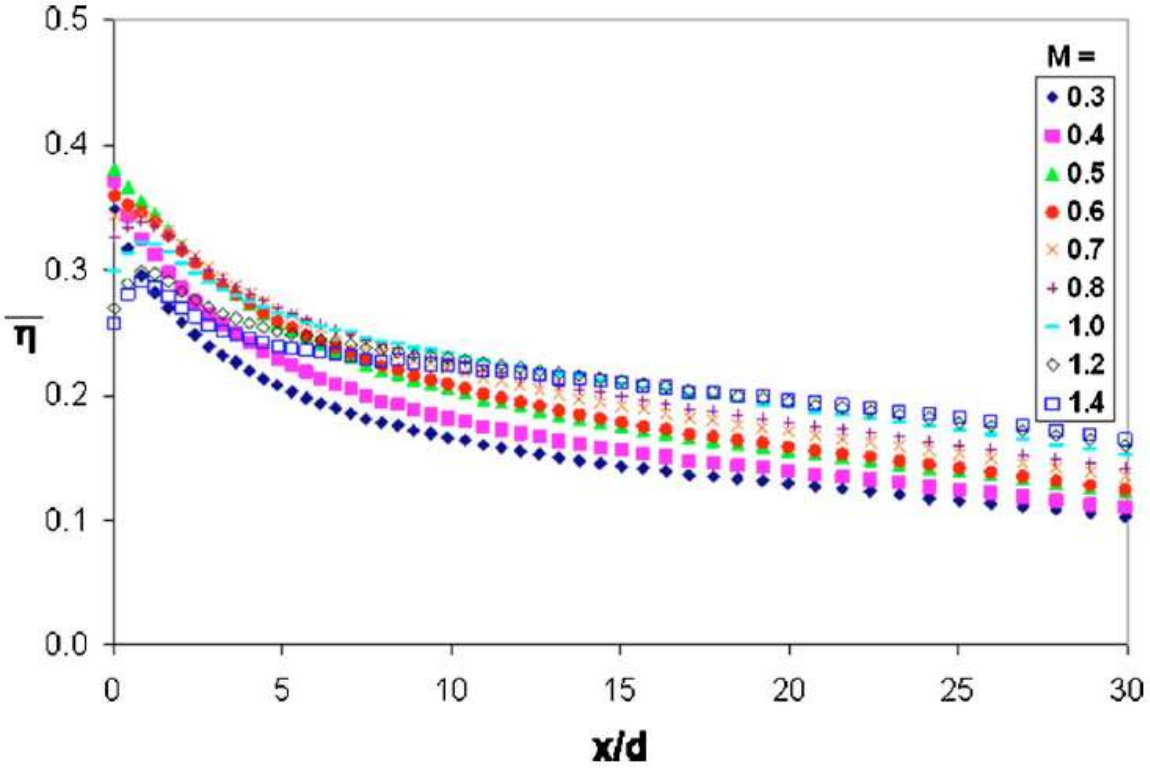

Figure 25 Laterally averaged adiabatic effectiveness for wide trench [15]

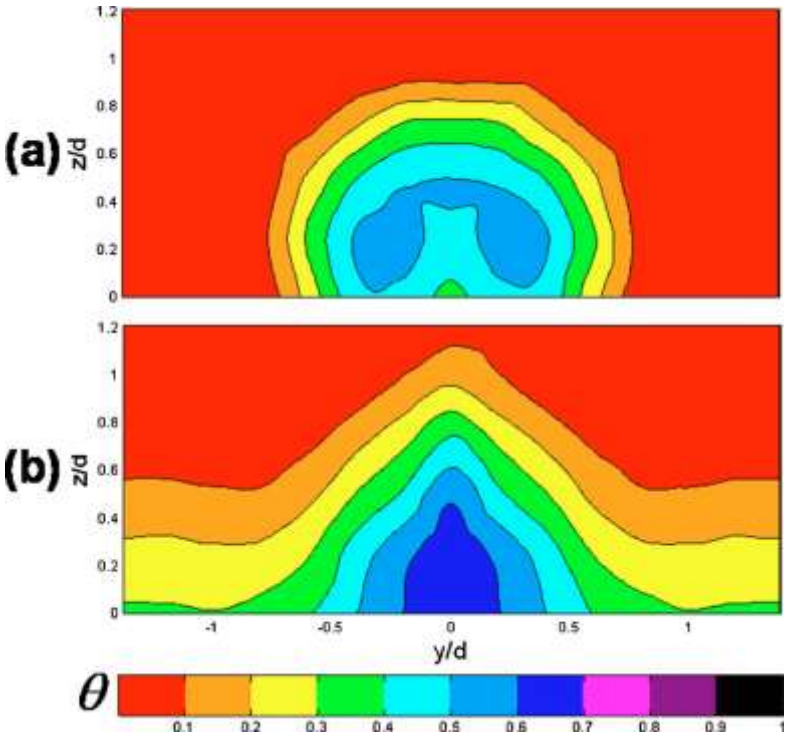

Figure 26 Thermal profiles for *a*) axial hole, and *b)* narrow trench configurations, *x*/*d*=2, *M*=1.0 [15]

5.3 Effect of blowing ratio on film cooling effectiveness

The value of the effectiveness decreases as the downstream distance increases. For-shaped hole and laidback shape hole data Waye and Bogard[15] referred Saumweber et al.[9] paper. For some of the blowing ratios, the narrow trench performed better than the fan-shaped holes, which can be confirmed from Fig.27.

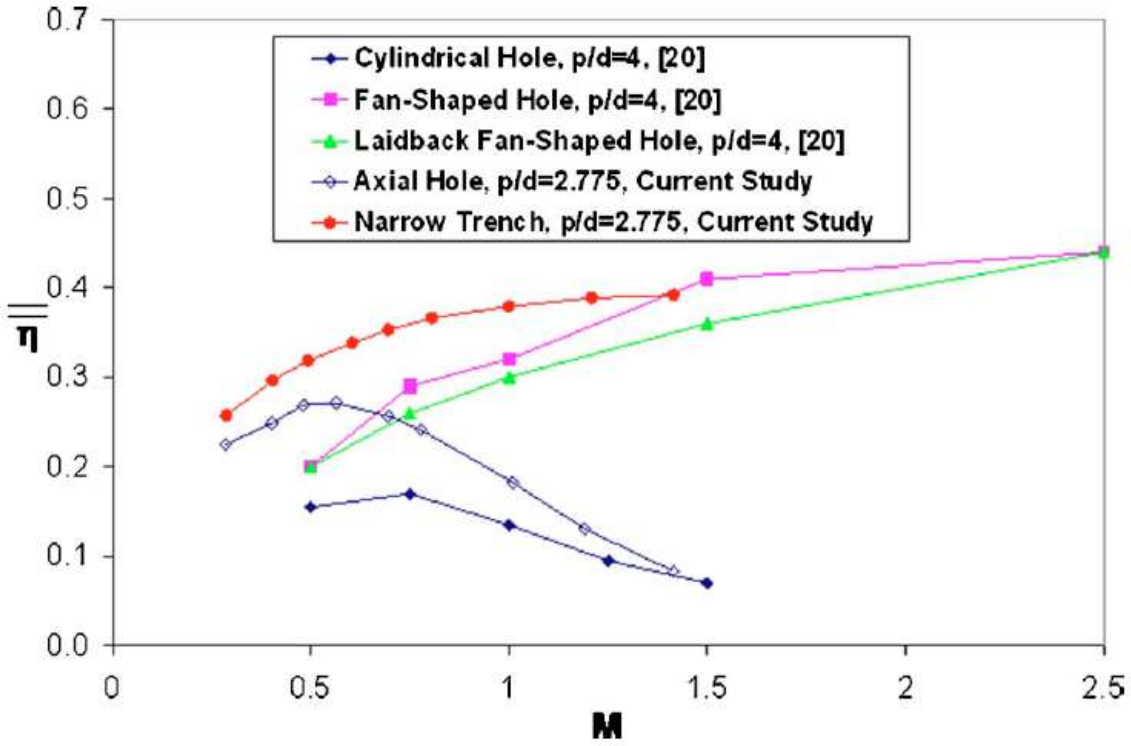

Figure 27 Comparison of total average effectiveness for axial holes, shaped holes, and narrow trench holes. [15]

5.4 Effect of alignment on film cooling effectiveness

Kianpour et al.[16] simulated Pratt and Whitney gas turbine engine to compare trenched hole and cylindrical hole configuration. The zero degree alignment is similar to the normal case of cylindrical holes if no sidewall was present. Sidewall obstructs the flow in the lateral direction and disturbs the vortex formed making the configuration better than the cylindrical holes. Separation of the coolant along the downstream at higher blowing ration can cause decrease in the effectiveness for the zero degree alignment.

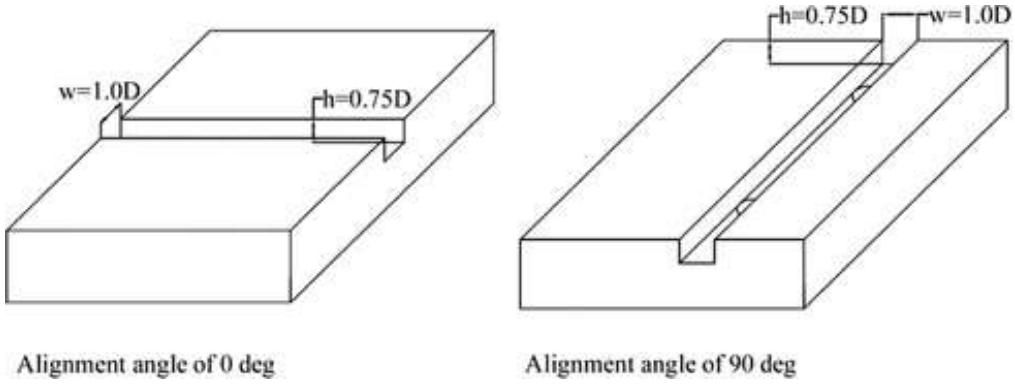

Figure 28 Arrangement of trenched cooling holes with different alignment angles. [16]

The configuration studied is by [16] is the optimum configuration of depth to diameter ratio which was reported by Lu et al.[14] (depth to diameter = 0.75). Kianpour et al.[16] have given the variation of adiabatic effectiveness with vertical distance measured from the exit of the hole to the end of the trench thus making it difficult to compare with the literature surveyed. The 90 degree configuration gives better effectiveness as the spreading of the coolant in lateral direction is not restricted contrary to the 0 degree case. Thus it is better to have the 90 degree alignment trench.

5.5 Numerical simulation

Antar et al.[17] analysed the narrow trench configuration using ANSYS CFX for the simulation. Three turbulence models SST Gamma Theta, k-ω and k-ε were used for the comparison of the data at the blowing ratio M=0.5 and X/D range of 5 to 40. The results for different models were validated with Sinha et al.[7] and Waye and Bogard[15] for different values of blowing ratios. Fig.29 shows the result for the variation of centreline effectiveness for the different models used with the same flow conditions. The data is predicted more effectively by the SST model inside the trench. At high blowing ratio, due to detachment of the jet, all the models report wrong data.

Peng and Jiang[4] simulated the experiment in Fluent software for cylindrical, shaped and trenched holes with 30 degree inclination angle. The trench hole configuration was too shallow as the depth to diameter ratio is 0.4 which is less than the minimum value of 0.577. The simulated data shown in Fig.30 shows temperature distribution and velocity vectors calculated at downstream distance X/D = 6 at blowing ratio of one.

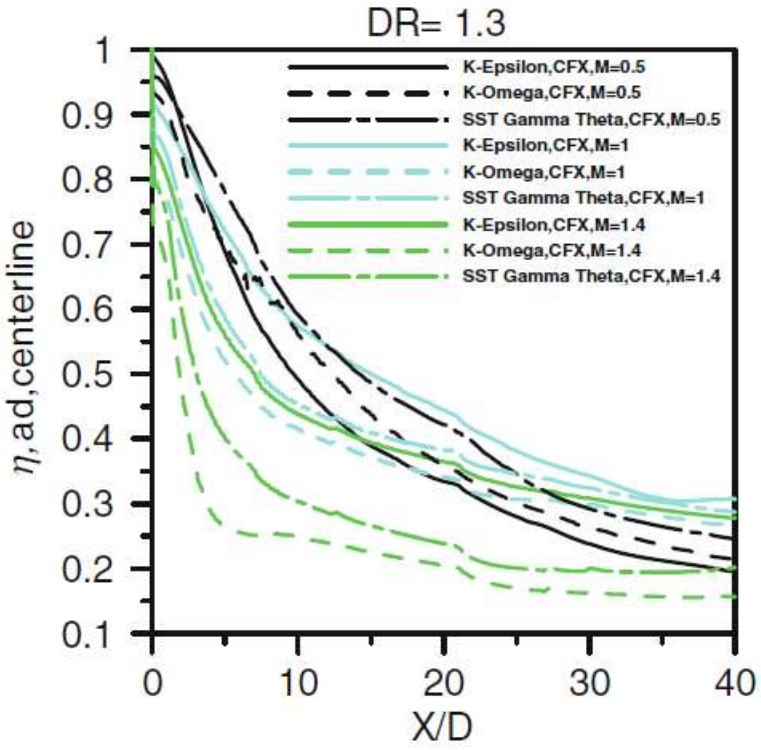

Figure 29 Centerline adiabatic film effectiveness at various blow ratios with three turbulence models for narrow trench [17]

Because of the less depth used by the authors, the counter-rotating vortex pair is not destroyed completely and thus can be seen in the Fig.30. The spreading of the coolant in lateral direction for trench holes is still better than the cylindrical holes. Plenum model has coolant injection in mainstream direction and cross flow model has coolant injection in perpendicular direction of the mainstream. Single vortex is formed because of the cross-flow injection. The CFD methods give deviation from the experimental data irrespective of the turbulence model chosen. This is because of the complexity of the flow near the airfoil surface. The CFD technique can be used to understand the flow physics but exact prediction of the temperature contours and velocity vectors is not possible.

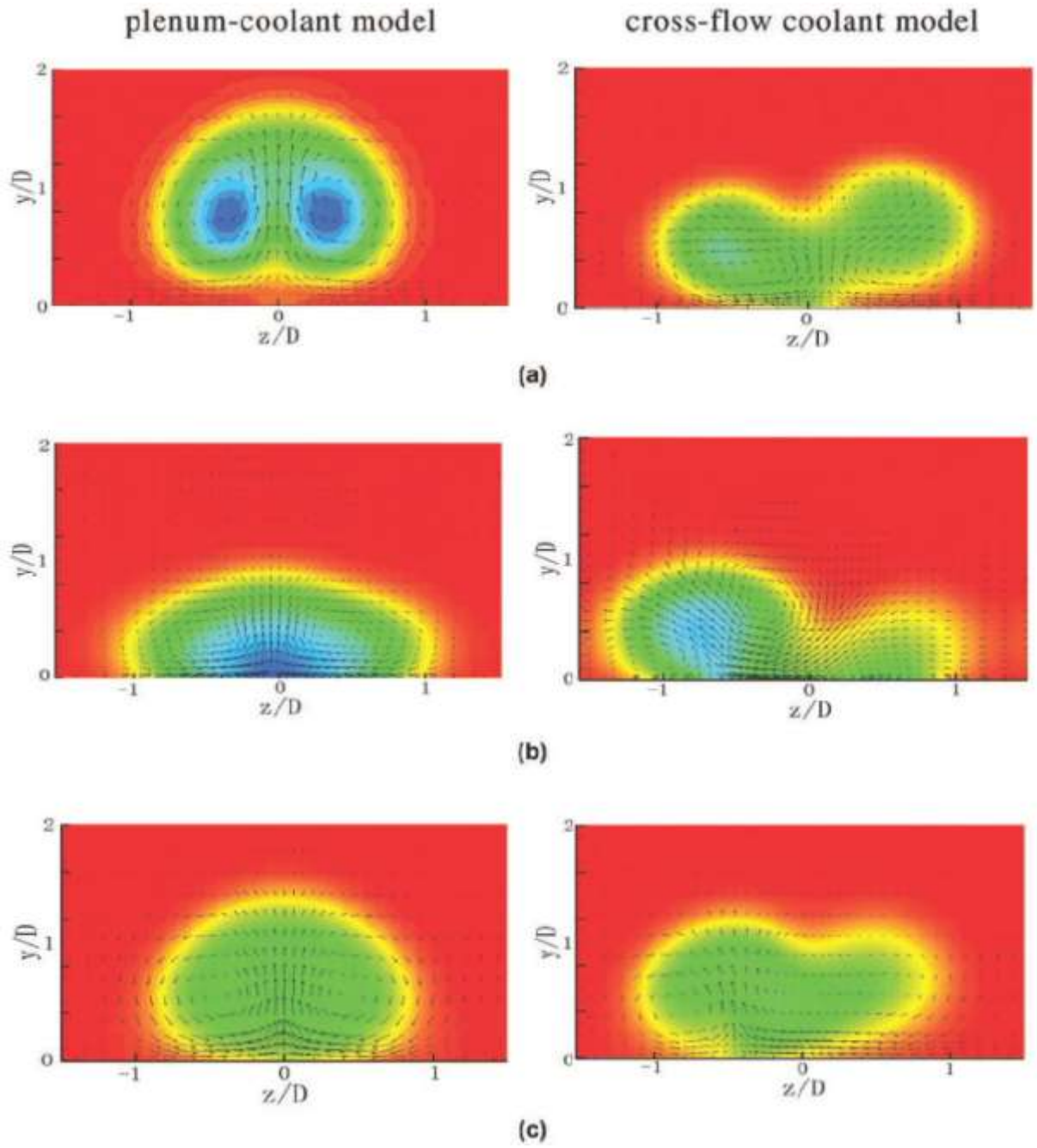

Figure 30 Predicted temperature and velocity distributions for X/D = 6 (M =1): (a) cylindrical hole, (b) fan-shaped hole, and (c) trenched hole

Chapter 6
CONCLUSION

Various parameters influence gas turbine film cooling, and it is vital to study their effect on cooling performance. The interaction between the coolant and the mainstream affects the performance of the system. The performance is quantified by film effectiveness, heat transfer coefficients, and net heat flux reduction. Many studies focus on the parameter film effectiveness alone. However, all the parameters are equally crucial for fully understanding the performance of film cooling.

Film cooling performance is affected the separation of the jet from the surface. The shaping of the hole exit, trench on the surface, turbulence intensity, blowing ratio has a significant effect on the separation and spreading of the coolant. It is clear from the results of Goldstein et al.[2] and Sinha et al.[7] that as the higher blowing ratio increased, the momentum of the coolant jet is increased causing it to separate from the surface. The separation can be understood by understanding the behaviour of the flow by CFD techniques. CFD predictions can provide excellent insight into spatial details of the flow process. However, the model chosen in numerical simulation is important as the results of Antar et al.[17] gave the trend of the flow parameters but the experiment values were not matched.

From the results of Waye and Bogard[15], it can be noted that the cylindrical hole is the basic configuration that can work for limited flow condition. Although the shaping the holes requires high manufacturing cost compared to the cylindrical holes it helps in better spreading of the coolant on the surface (Fig.30) making it more effective than the cylindrical holes. The trenched hole is an extension of slot configuration and has simple design compared to the shaped holes. With thermal barrier coating, the trenched hole configuration can give comparable and even better results for some blowing ratios [15]. It is observed that the geometry of the trench has a high influence on the performance of the film cooling. A narrow and shallow trench is preferable for better performance [14, 15]. In summary, the advantages of a particular configuration and flow pattern should be considered while deciding the numerical and experimental technique for the determination of film effectiveness and the optimum design of the film cooling arrangement. The trench configuration with intermittent slots is not reported in any literature so far. It can be studied to check the feasibility of the intermittent slot and hole configuration.

REFERENCES

[1] D.G. Bogard, K.A. Thole, “Gas Turbine Film Cooling,” J. Propuls. Power. 22 (2006) 249–270. doi:10.2514/1.18034

[2] R.J. Goldstein, E.R.G. Eckert, F. Burggraf, “Effects of hole geometry and density on three-dimensional film cooling,” Int. J. Heat Mass Transf. 17 (1974) 595–607. doi:10.1016/0017-9310(74)90007-6

[3] M. Gritsch, W. Colban, H. Schär, K. Döbbeling, “Effect of Hole Geometry on the Thermal Performance of Fan-Shaped Film Cooling Holes,” J. Turbomach. 127 (2005) 718. doi:10.1115/1.2019315

[4] W. Peng, P.X. Jiang, “Experimental and numerical study of film cooling with internal coolant cross-flow effects,” Exp. Heat Transf. 25 (2012) 282–300. doi:10.1080/08916152.2011.609630

[5] E. Lutum, B. V. Johnson, “Influence of the Hole Length-to-Diameter Ratio on Film Cooling With Cylindrical Holes,” J. Turbomach. 121 (1999) 209. doi:10.1115/1.2841303

[6] D.R. Pedersen, E.R.G. Eckert, R.J. Goldstein, “Film Cooling With Large Density Differences Between the Mainstream and the Secondary Fluid Measured by the Heat-Mass Transfer Analogy,” J. Heat Transfer. 99 (1977) 620. doi:10.1115/1.3450752

[7] A.K. Sinha, D.G. Bogard, M.E. Crawford, “Film-Cooling Effectiveness Downstream of a Single Row of Holes With Variable Density Ratio,” J. Turbomach. 113 (1991) 442. doi:10.1115/1.2927894

[8] B. Johnson, K. Zhang, W. Tian, H. Hu, “An Experimental Study of Film Cooling Effectiveness by Using PIV and PSP Techniques,” J. Turbomach. (2013). doi:doi:10.2514/6.2015-0352

[9] C. Saumweber, A. Schulz, S. Wittig, “Free-Stream Turbulence Effects on Film Cooling With Shaped Holes,” J. Turbomach. 125 (2003) 65. doi:10.1115/1.1515336

[10] E. Lutum, J. von Wolfersdorf, B. Weigand, K. Semmler, “Film cooling on a convex surface with zero pressure gradient flow,” Int. J. Heat Mass Transf. 43 (2000) 2973–2987. doi:https://doi.org/10.1016/S0017-9310(99)00346-4

[11] J.H. Leylek, R.D. Zerkle, “Discrete-Jet Film Cooling: A Comparison of Computational Results With Experiments,” \Jtu. 116 (1994) 358–368

[12] B.A. Haven, M. Kurosaka, “Kidney and anti-kidney vortices in crossflow jets,” J. Fluid Mech. 352 (1997) 27–64. doi:10.1017/S0022112097007271

[13] R.S. Bunker, “Film Cooling Effectiveness Due to Discrete Holes Within a Transverse Surface Slot,” Vol. 3 Turbo Expo 2002, Parts A B. (2002) 129–138. doi:10.1115/GT2002-30178

[14] Y. Lu, A. Dhungel, S. V. Ekkad, R.S. Bunker, “Effect of Trench Width and Depth on Film Cooling From Cylindrical Holes Embedded in Trenches,” Vol. 4 Turbo Expo 2007, Parts A B. 131 (2007) 339–349. doi:10.1115/GT2007-27388

[15] S.K. Waye, D.G. Bogard, “High Resolution Film Cooling Effectiveness Measurements of Axial Holes Embedded in a Transverse Trench With Various Trench Configurations,” Vol. 3 Heat Transf. Parts A B. 2006 (2006) 205–213. doi:10.1115/GT2006-90226

[16] E. Kianpour, N.A.C. Sidik, I. Golshokouh, “Measurement of film effectiveness for cylindrical and row trenched cooling holes at different blowing ratios,” Numer. Heat Transf. Part A Appl. 66 (2014) 1154–1171. doi:10.1080/10407782.2014.901042

[17] A. Antar, Z. Qun, E. Fifi, “Aerodynamic analysis and validation by using three turbulence models for narrow trench configuration,” Heat Mass Transf. Und Stoffuebertragung. 50 (2014) 603–616. doi:10.1007/s00231-013-1261-5